AD-A193 901 CORROSION CONTROL THROUGH A BETTER UNDERSTANDING OF THE 1/1
METALLIC SUBSTRAT..(U) LEHIGH UNIV BTTHLEHEM PA
ZETTLEMOYER CENTER FOR SURFACE STUDI..
UNCLASSIFIED H LEIDHEISER ET AL. 04 JAN 88 F/G 11/3 NL

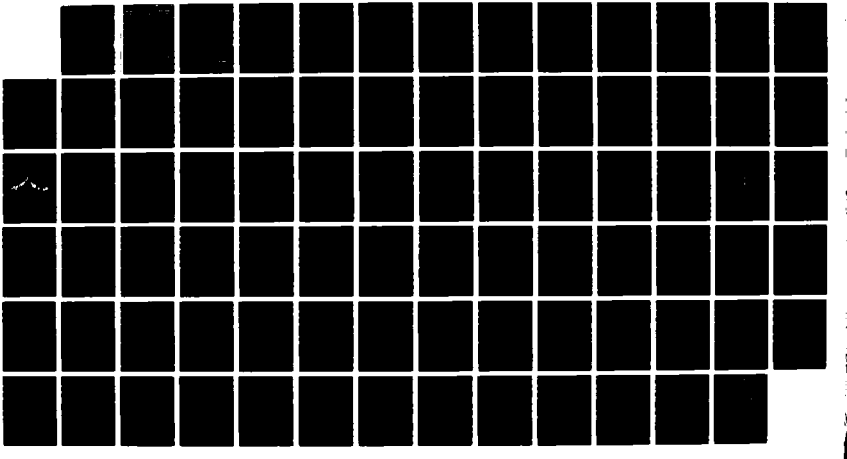

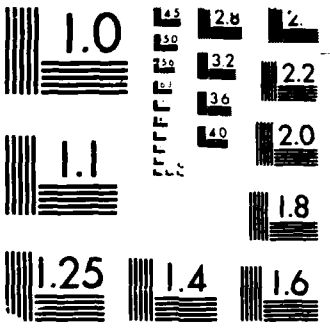

(4)

CORROSION CONTROL THROUGH A BETTER UNDERSTANDING OF THE METALLIC SUBSTRATE/ORGANIC COATING/INTERFACE

Agreement No. N00014-79-C-0731

EIGHTH ANNUAL REPORT
COVERING THE PERIOD

OCTOBER 1, 1986 - SEPTEMBER 30, 1987

Sponsor: Office of Naval Research
Washington, D.C.

Principal Investigator: Henry Leidheiser, Jr.
Co-Investigator: Richard D. Granata

Zettlemoyer Center for Surface Studies
LEHIGH UNIVERSITY
Bethlehem, PA 18015

January 4, 1988

TABLE OF CONTENTS

FOREWORD

This report represents the eighth annual summary of research carried out under Office of Naval Research Contract No. N000014-79-C-0731. The objective of this research is to obtain a better understanding of the metallic substrate/organic coating/interface system so that improvements may be made in corrosion control of metals by painting.

Papers published during the period, January 1, 1987 - December 31, 1987, for which ONR provided total or partial financial support are listed chronologically.

Four summaries of reports representative of work completed during the past year are given. Three of these papers have been accepted for publication and one paper will be published in a proceedings volume of the American Chemical Society.

Papers Covering Work Supported by ONR and Published during 1987

"Inhibition of the Oxygen Reduction Reaction using 8-Hydroxyquinoline," H. Leidheiser, Jr., H. Konno, and A. Vértes, CORROSION 43, 45-50 (1987).

"COATINGS," Henry Leidheiser, Jr., In Corrosion Mechanisms, ed. F. Mansfeld, Marcel Dekker: New York, 1987, pp. 165-209.

"The Permeability of a Polybutadiene Coating to Ions, Water and Oxygen," Henry Leidheiser, Jr., Douglas J. Mills, and Wayne Bilder, In Proceedings of the Symposium on Corrosion Protection by Organic Coatings, Eds. M. W. Kendig and H. Leidheiser, Jr., ECS Vol. 87-2, 1987, pp.23-36.

"The Activation Energy for Cathodic Delamination of Polybutadiene from Steel in Chloride Solutions," Henry Leidhesier, Jr., and John Catino, In Proceedings of the Symposium on Corrosion Protection by Organic Coatings, Eds. M.W. Kendig and H. Leidheiser, Jr., ECS Vol. 87-2, 1987, pp.126-39.

"Electrochemical Studies of Uncoated and Polymer-Coated Abrasively-Blasted Mild Steel," H.E. George Rommal and Henry Leidheiser, Jr., In Proceedings of the Symposium on Corrosion Protection by Organic Coatings, Eds. M.W. Kendig and H. Leidheiser, Jr., ECS Vol. 87-2, pp.126-39.

"Resistance Measurements of Organic Coatings as a Means for Evaluating Corrosion Protection in Acid Solutions," Malcolm L. White, Douglas J. Mills and Henry Leidheiser, Jr., In Proceedings of the Symposium on Corrosion Protection by Organic Coatings, Eds. M.W. Kendig and H. Leidheiser, Jr., ECS Vol. 87-2, 1987, pp.208-16.

"Emission Mössbauer Studies of Sn^{+4} Introduced into Corrosion Protective Coatings by Cathodic Polarization," Henry Leidheiser, Jr., Attila Vértes, Ilona Czakó-Nagy, and József Farkas, J. Electrochem. Soc. 134, No. 4, 823-25 (1987).

"Positron Annihilation Behavior in Several Corrosion Protective Coatings," Henry Leidheiser, Jr., Csaba Szeles and Attila Vértes, Nuclear and Instrument Methods in Physics Research A255, 606-10 (1987).

"Whitney Award Lecture--1983, 'Towards a Better Understanding of Corrosion Beneath Organic Coatings,'" Henry Leidheiser, Jr., In Office of Naval Research, Forty Years of Excellence in Support of Naval Science, Anniversary 1946-86, Department of the Navy: Arlington, VA, pp.311-24. (Reprint of Corrosion 39(5), 189-201 (1983).

"Technical Note: Alkali Metal Ions as Aggressive Agents to Polymeric Corrosion Protective Coatings," H. Leidheiser, Jr., R. D. Granata, and R. Turoscy, Corrosion 43(5), 296-97 (1987).

"Emission Mössbauer Study of Cobalt Ions in an Organic Coating," Henry Leidheiser, Jr., Ilona Czakó-Nagy and Attila Vértes, J. Electrochem. Soc. 134(6), 1470-72 (1987).

"Water Disbondment and Wet Adhesion of Organic Coatings on Metals: A Review and Interpretation," H. Leidheiser and W. Funke, JOCCA 70(5), 121-49 (1987).

Publications (Cont'd.)

"Cathodic Delamination of Polybutadiene from Steel -- A Review," Henry Leidheiser, Jr., J. Adhesion Sci. Tech. 1(1), 79-98 (1987).

"Corrosion Behavior of Steel Pre-treated with Silanes," H. Leidheiser, Jr., M. De Crosta, and R. D. Granata, CORROSION 43(6), 382-87 (1987).

"Corrosion Inhibited Metal," Henry Leidheiser, Jr., and Hidetaka Konno, Patent Number 4,681,814, July 21, 1987.

"Emission Mössbauer Study of the Interface Between a Cobalt Substrate and a Polyimide Coating," Attila Vértes, Ilona Czakó-Nagy, Philip Deck and Henry Leidheiser, Jr., J. Electrochem. Soc. 134(7), 1628-32 (1987).

"Positron Implantation in Polymer Coatings," K. Süvegh, Cs. Szeles, A. Vértes, M. L. White and H. Leidheiser, Jr., J. Radioanal. Nucl. Chem., Letters 117(3), 183-93 (1987).

Ion Transport through Protective Polymeric Coatings When Exposed to an Aqueous Phase

Henry Leidheiser, Jr., and Richard D. Granata

Note: This paper has been accepted for publication in THE IBM JOURNAL OF RESEARCH AND DEVELOPMENT

Ion Transport through Protective Polymeric Coatings
When Exposed to An Aqueous Phase

ABSTRACT

This paper describes the status of work in our laboratory to develop an improved understanding of the chemical and physical aspects of ion transport through polymeric coatings when exposed to an aqueous phase.

INTRODUCTION

Protective polymeric coatings for metal and electrical component surfaces are designed primarily to serve as barriers for environmental constituents such as water, oxygen and other atmospheric gases, and ions. Water permeation is undesirable because liquid phase development at the metal/polymer interface may lead to water disbondment (1) or to corrosion. Oxygen permeation is undesirable because oxygen is a component of the cathodic half of the corrosion reaction which may occur in the aqueous phase under the coating. Ion permeation is undesirable because ions are the charge carriers in polymeric coatings and processes such as corrosion or short circuiting are dependent on charge transport.

Many biological processes are dependent on ion tranport through membranes and many afflictions of humans are caused by perturbations in the normal ion transport processes. However, in this paper, we limit our discussions to the transport of ions through neat resin or formulated coatings that range in thickness from 3 to 7500 μm.

Our interest in ion transport thorugh polymeric coatings developed as a consequence of studies of the phenomenon of cathodic delamination [2]. This term is applied to the consequences of the application of a cathodic potential to a metal having a perforated coating while the system is immersed in an electrolyte. The phenomenon is important because of the use of cathodic protection to reduce corrosion of coated pipelines, ships and chemical processing vessels. Our studies led us to the conclusion that the rate of delamination of the coating in the presence of the applied cathodic potential was determined by the rate of ionic migration thorugh the coating. This conclusion met resistance from two generations of graduate students but most of them accepted it as they pursued research on the phenomenon of cathodic delamination. Our interest then turned to understanding the process by which ions move through a coating and the chemical nature of an ion when present within a coating matrix. The ion transport process with which we will be concerned is that which occurs when the polymeric coating is in contact with an aqueous phase containing an ion concentration of 0.001M or greater. The ion transport process may occur in the absence or presence of an externally applied potential. Three aspects of ion transport will be discussed in this report: (a) methods used in our laboratory to measure ion transport; (b) the morphology of polymeric coatings as related to ion transport; and (c) the chemical nature of an ion in a coating.

The presence and behavior of ionic groups in polymers have been extensively studied. A symposium on this subject is a good reference [3]. Polymeric coatings differ from ionic polymers in that they generally contain relatively few ionic groups, are used in thin film form, are applied to a solid substrate, contain pigments, fillers and other components, are often applied as a solution or a dispersion, and are formed on the solid surface by many different techniques. These unique characteristics of a coating, as opposed to a neat polymer, place added emphasis on the morphology of the coating and the effect of this morphology on ion transport.

MEASURING ION TRANSPORT THROUGH A COATING

Four techniques have been used in our studies: DC measurements, electrochemical impedance spectroscopy, under-the-coating sensing and radiotracer measurements. Some of the results obtained using each of these techniques will be described.

DC Measurements. The classic work of Bacon, Smith and Rugg [4] and more recent studies [5] have shown that high resistances (>10^9 ohm·cm²) of the coating are associated with good corrosion protection and low resistances (<10^7 ohm·cm²) are associated with poor corrosion protection. This representation (ohms·cm²) of the coating resistance is given in terms of the resistance of a cm² section of the coating. The thickness of the coating is not taken account of in this value. This generalization appears to hold true when coatings are exposed to 0.5M NaCl solutions but does not appear to hold true in dilute alkali chloride solutions [6]. The reasons for this latter inconsistency will become apparent in the discussions which follow.

Mayne and Mills [7] were the first to point out that coatings exhibit two types of electrical behavior when immersed in ionic solutions. In the first case, to which the term "I-type" has been applied, the coating (or the free film) has a high resistance and the resistance of the coating is inversely proportional to the resistance of the electrolyte with which it is in contact. In the second case, to which the term "D-type" has been applied, the resistance of the coating is low and is directly proportional to the resistance of the electrolyte with which it is in contact. An example of this type of behavior for a 25 μm thick polybutadiene coating is shown in Figure 1 [8]. It is interesting to point out that different sections of the same coating may be I-type or D-type. In the original work of Mayne and Mills, 11 of the 25 one cm² sections had DC resistances of 10^8 ohm·cm² or less (D-type) and 14 had DC resistances of 10^{11} ohm·cm² or greater (I-type).

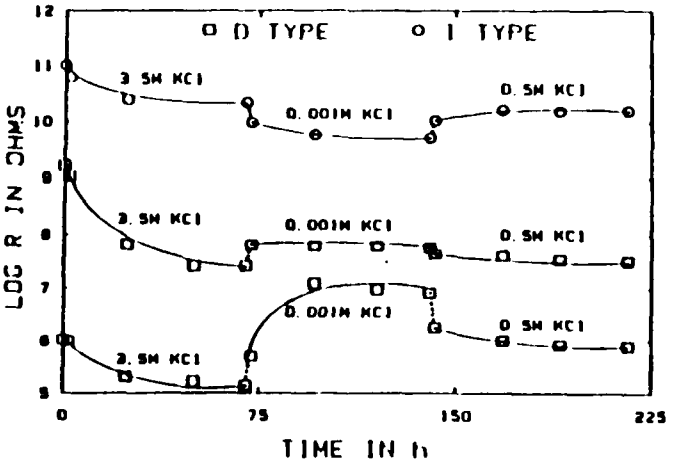

Figure 1. The effect of changing the solution concentration on the resistance of a 25 μm thick polybutadiene film. From [8], reproduced with permission of The Electrochemical Society.

Coatings exhibit "I" behavior when there are no continuous aqueous pathways through the coating. Water ingress or egress is then controlled largely by the relative thermodynamic activities of water within the polymer and within the electrolyte. In the case of coatings exhibiting "D" behavior, aqueous pathways through the coating exist and the aqueous phase within these pathways equilibrates with the bulk electrolyte.

The above work, as well as additional work done by Mills in our laboratory [9] shows that the ion transport process in coatings is not homogeneous, that there are regions where ion transport occurs with a high resistance, and other regions where ion transport occurs with a relatively low resistance.

The resistances of the majority of thin film coatings decrease with time of exposure to alkali metal solutions as shown by the data in Figure 2 where the resistance of a polybutadiene coating is seen to decrease from a value in excess of 10^{11} ohms·cm^2 to approximately 10^7 ohm·cm^2 when the coating was immersed in 1M NaOH at 60°C for 5 days. The sensitivity of the resistance to the electrolyte in contact with the coating is also shown in the same figure where it will be noted that the resistance decreased in any solution containing Na^+ or K^+ ions but could be brought back to its original value upon immersion in a solution containing H^+ ions. It is apparent from these measurements that the coating is permeable to ions and that the type of ions present in the electrolyte controls the ability of the coating to transport charge. The increased charge transport capability of some coatings in the presence of alkali metal ions is an interesting phenomenon.

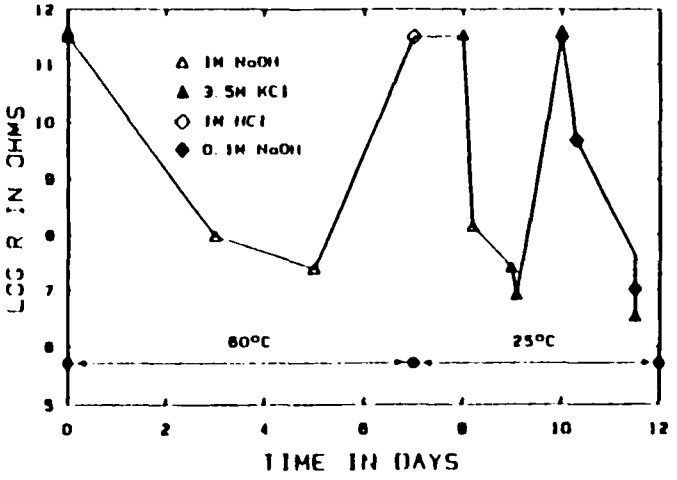

Figure 2. The change in resistance of an I-type polybutadiene film, 35 μm in thickness, when exposed to different ionic solutions. From [8], reproduced with permission of The Electrochemical Society.

Electrochemical Impedance Spectroscopy. In the absence of active corrosion at the metal/coating interface, the coating may be characterized simplistically as a resistor and a capacitor in parallel. This circuit is in turn in series with a resistor representing the resistance of the solution. Typical impedance spectra for sections of the polybutadiene coating whose behavior was outlined in Figure 1 are given in Figure 3 in a Bode plot representation. The I-type section of the film exhibits a simple capacitance-like behavior with a -1 slope over the range of frequency examined, whereas the D-type sections show a plateau region at low frequencies; the plateau is characteristic of a resistor. The impedance value at 10^{-3} Hz is approximately the same as the value of the DC resistance.

Changes in the impedance spectra with time of exposure to an electrolyte have been very useful in characterizing the protective properties of the coating [10-12]. An example of the changes in the spectrum with time is given in the Bode plot shown in Figure 4. The plateau at the low frequency is the sum of the resistance of the coating and the resistance of the electrolyte. The latter value is very small in comparison to the resistance of the coating and thus the changes are a consequence of the change in resistance of the coating. Such measurements show that as corrosion proceeds, the low-frequency impedance decreases in value indicative of the fact that ion passage through the coating is facilitated in concert with the deterioration of the protective properties of the coating.

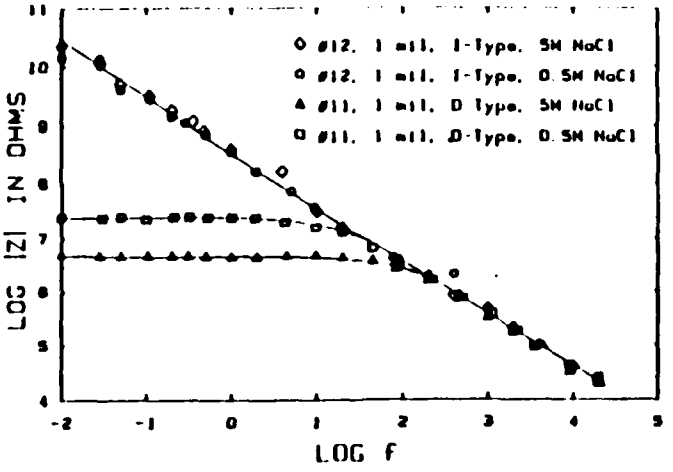

Figure 3. Bode plots for I- and D-type polybutadiene coatings on steel exposed to two different concentrations of NaCl. From [8], reproduced with permission of The Electrochemical Society.

The impedance spectrum of some coatings is especially sensitive to temperature. An example is given in Figure 5 for an epoxy coating whose impedance spectra were determined in 0.5M NaCl as a function of temperature. Note that the room temperature impedance at low frequency was of the order of 10^9 ohm·cm^2 and it progressively decreased in value with increase in temperature until it reached approximately 10^5 ohms·cm^2 at 80°C. An interesting feature of these experiments is the fact that the low frequency impedance returned to its original value when the system was cooled to room temperature at the conclusion of the experiment. In contrast, some high impedance coatings exhibit little change in immpedance when exposed to distilled water over a temperature range of 25-80°C.

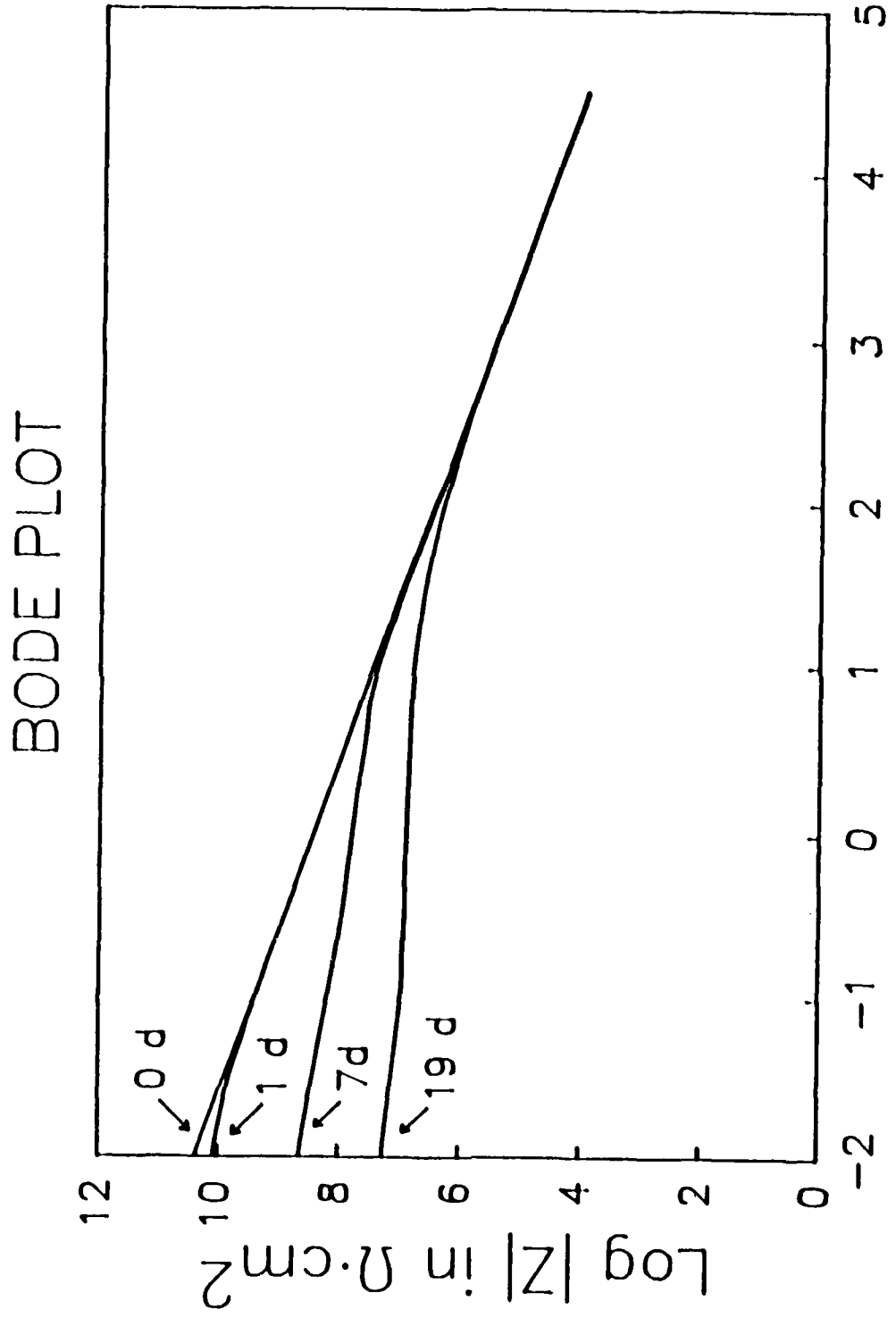

Figure 4. Changes in impedance spectra for different times of exposure to an aggressive electrolyte.

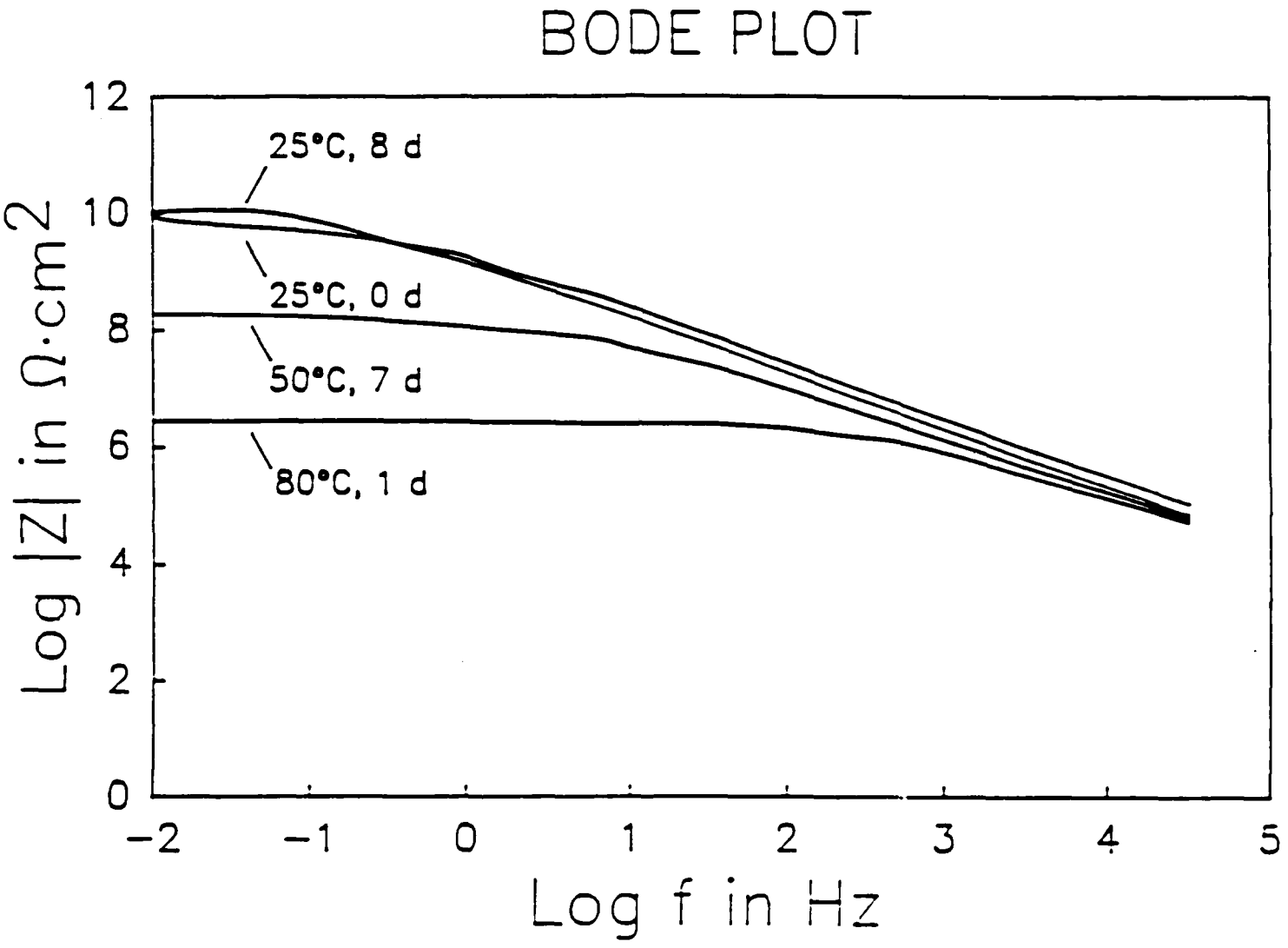

Figure 5. The impedance spectrum of an epoxy coating on steel while immersed in 0.05M NaCl under different experimental conditions.

Under the Coating Sensing. Vedage [13] has utilized a sensor beneath a coating to determine the rate at which ions pass through a coating. She inserted an insulated, iridized titanium electrode through small holes drilled in a steel substrate, applied the coating and measured the pH electrochemically against a standard electrode immersed in the same solution to which the coating was exposed. This procedure provided two kinds of information. There was no electrical response until sufficient conductivity developed in the vicinity of the pH electrode. The onset of conductivity determined the time required for water to pass through the coating and to establish a conducting matrix. Changes in the potential were used to determine the changes of the pH of the conducting phase in the vicinity of the electrode. Measurements were made with four coatings: a polyester, an epoxy, a fluoropolymer and a vinyl ester while immersed in 0.1M H_2SO_4 at 60°C. The pH which the electrode sensed as a function of time is given for three of the four coatings in Figure 6. Note that the polyester coating exhibited a low pH beneath the coating after 1 day immersion whereas the vinyl ester coating required approximately 45 days before the pH under the coating achieved a low value.

Vedage also used the blistering rate of an epoxy polyamideamine coating to determine the rate of diffusion of hydrogen ions through the coating. She determined the time to first blister as a function of coating thickness and calculated a diffusion coefficient from a plot of time to first blister vs the square root of the thickness of the coating. Values of the calculated diffusion coefficient when the coated steel was immersed in various electrolytes at 60°C are given in Table I.

Table I

Calculated Diffusion Coefficients for Hydrogen Ions Diffusing through an Epoxy Polyamideamine Coating on Steel

Electrolyte	Calculated Diffusion Coefficient ($cm^2\ sec^{-1}$)
0.5M H_2SO_4	6.5×10^{-9}
0.1M H_2SO_4	2.1×10^{-9}
0.1M H_2SO_4 + 0.5M Na_2SO_4	5.6×10^{-10}

It is clear from Table I that the diffusion coefficient of the hydrogen ion based on blistering data was less in the presence of Na_2SO_4 than in pure H_2SO_4 of the same molarity. A study was then made of the rate of blistering as a function of the addition of other sulfates to the sulfuric acid solution. Foreign ions had major effect on the rate of blistering as can be noted from the data in Table II.

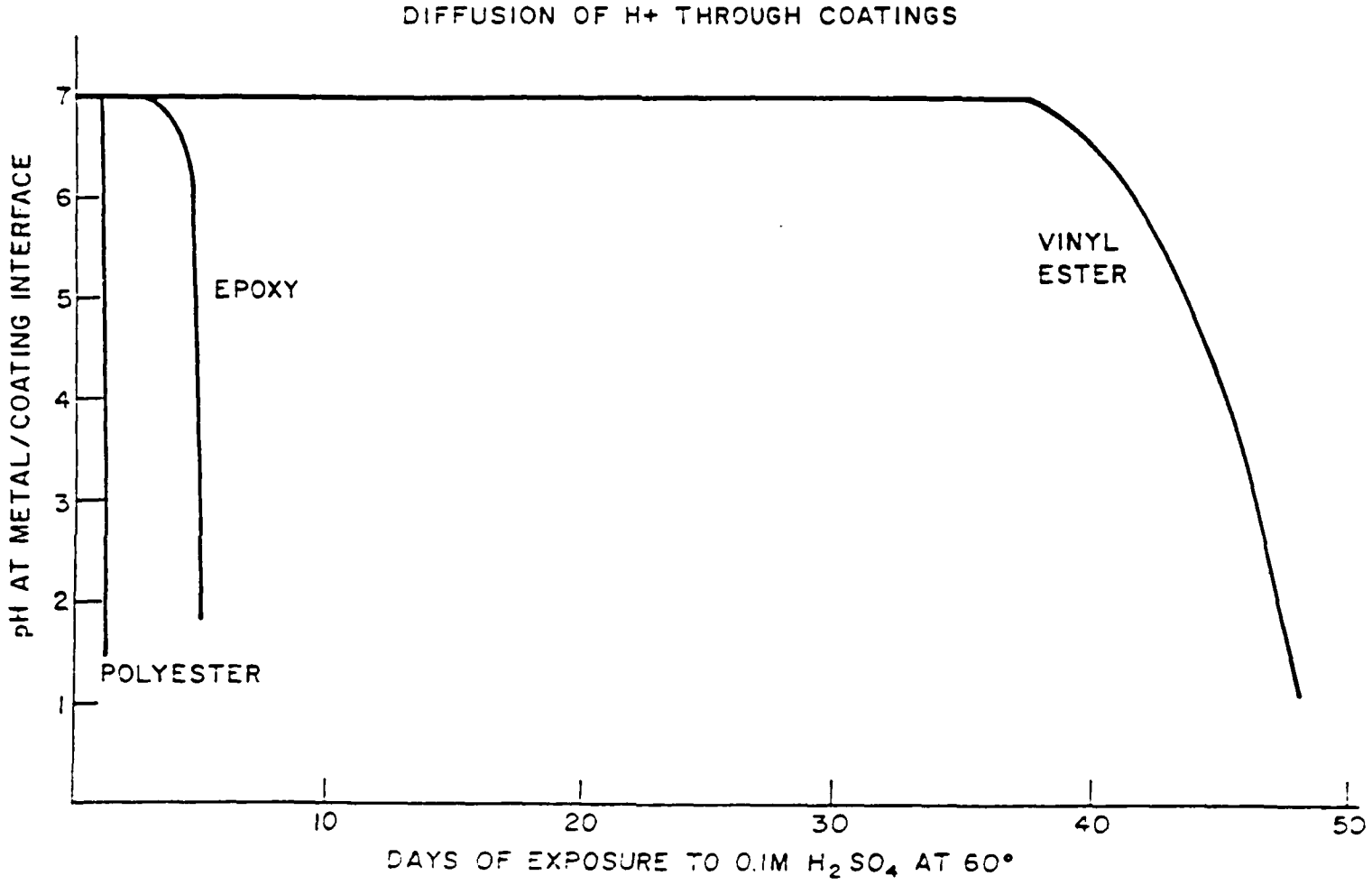

Figure 6. The pH beneath a coating as a function of time of exposure to 0.1M H_2SO_4 at 60°C [13].

Table II
The Rate of Blistering of a 0.6 mm Thick Epoxy Polyamideamine Coating when Immersed in 0.1M H_2SO_4 Containing Other Sulfates

Electrolyte	Approximate Time to Blister (h)
0.1M H_2SO_4	60
0.1M H_2SO_4 + 0.5M Li_2SO_4	150
0.1M H_2SO_4 + 0.5M Na_2SO_4	300
0.1M H_2SO_4 + 0.5M K_2SO_4	425
0.1M H_2SO_4 + 0.5M $SnSO_4$	75
0.1M H_2SO_4 + 0.5M $MgSO_4$	150

These data suggest that the second ion competes for diffusion sites within the coating and reduces the rate at which the hydrogen ion can diffuse through the coating. This competition for sites also appears to depend on the size of the hydrated ion, with the larger ions such as $Li(H_2O)_x^+$ having only a small effect relative to the smaller $K(H_2O)_y^+$ ion. The relative behavior of these ions in affecting the blistering is additional circumstantial evidence that the ions diffusing through the coating are hydrated.

Radiotracer Measurements. Many studies have been carried out of the migration of species through a coating using radiotracer techniques. See for example the citations in reference [14]. Our remarks will be limited to our own studies which focused on the effect of an applied potential. Parks [14] measured the migration of radiotracer sodium and cesium ions through three different types of coatings on steel under both open-circuit conditions and an applied cathodic potential. As can be seen in Table III, the migration coefficient was approximately 10 times greater under those conditions where a small cathodic potential was applied than under open-circuit conditions. The term "migration coefficient" rather than "diffusion coefficient" is used because the application of a potential results in a migration that is not based solely on diffusion. The cathode potential of -0.8 V vs SCE represents a driving force of approximately -0.2 V.

Table III

The Effect of an Applied Potential on the Migration Coefficient of Two Cations in Three Organic Coatings

Coating System	Applied Potential	Migration Coefficient (cm^2/h)	
		Na^+	Cs^+
Alkyd top coat	none	4.6×10^{-8}	8.9×10^{-8}
	-0.2V	3.5×10^{-7}	5.7×10^{-7}
Alkyd top coat	none	3.2×10^{-9}	2.0×10^{-9}
+ primer	-0.2V	4.7×10^{-8}	3.2×10^{-8}
Polybutadiene	none	1.8×10^{-9}	1.7×10^{-9}
	-0.2 V	3.7×10^{-8}	2.0×10^{-8}

MORPHOLOGY OF ORGANIC COATINGS

The morphological features that are our concern in the present context are those that affect ion transport. The foregoing electrical measurements suggest that ion transport takes place through polymeric coatings by two different mechanisms. In those cases where the impedance at low frequencies is very high and where capacitive behavior is observed to frequencies of 10^{-3} Hz or less, it is likely that charge transport by cations occurs through the polymer matrix by a random walk process. The transport process involves the migration of cations through the matrix into dynamic free volumes caused by thermal motion of polymer segments. The transport involves the matrix as a whole with no continuous pathways of easy migration. Circumstantial evidence in support of this mechanism comes from the work of Turoscy and Granata [6] who observed that polybutadiene coatings on steel immersed in dilute chloride solutions corroded uniformly over the entire substrate even though the impedance remained as high as 10^9 ohm·cm^2. Under normal circumstances in 0.5M NaCl the corrosion process is highly localized [15] and the impedance is in the 10^6 ohm·cm^2 range. It appears that high concentrations of Na^+ degrade the barrier properties of polybutadiene. This degradation may come about through an effect of the Na^+ ions on carboxyl groups that are present in the uncured polymer and/or are formed during the oxidative curing process. Infrared spectra of polybutadiene after different amounts of curing [16] are given in Figure 7.

The low impedance coatings, as stated above, generally lose their protective properties in a highly localized manner. This low value of the impedance and the nature of the corrosion process lead us to believe that ion transport under these conditions occurs largely through continuous pathways through the polymer coating. The dimensions of these pathways and their geometry within the coating are unknown, although it is suspected that they have diameters before immersion in the electrolyte of the order of 1-10 nm. Once the corrosion process starts, local changes in the pH or in the ion concentration within the pathway lead to degradation of the coating and an increase in the diameter of the pathway or an improvement in the continuity of the pathway.

Coatings that retain solvent may also affect the pathways by introducing stresses in the coating. Such effects appear to be very important in the case of retained solvents, such as the glycol ethers, that are hydrophilic in nature and that develop local stresses when osmotic forces, caused by thermodynamic activity gradients, result in the enlargement of minute aggregates of the retained solvent.

Thus, in summary, the electrical measurements are best interpreted in terms of two charge transport paths, one through the matrix and the other through continuous pathways of small dimension. These two mechanisms suggest that a sodium ion, for example, should be present in the coating in two different environments, one in which its neighbors are part of the polymer matrix and the other in which it exhibits the properties of an ion in aqueous solution. A natural method for testing these conclusions is nuclear magnetic resonance (NMR) spectroscopy, since this technique is very sensitive to very small differences in the energy state of atoms as determined by the near

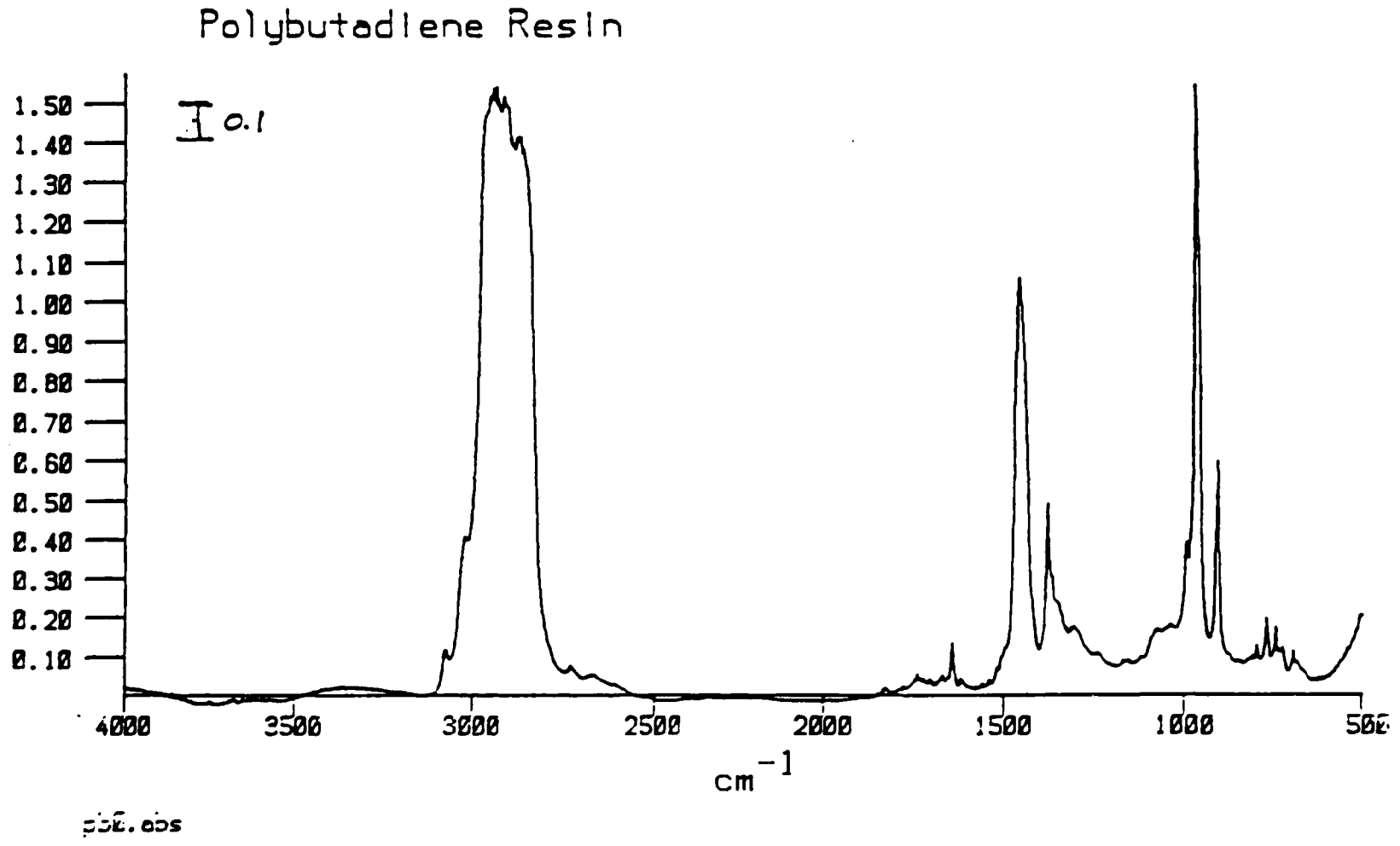

Figure 7(a). Infrared spectra of a polybutadiene resin coating after different amounts of curing in air at 200°C [16]: (a) before curing; (b) after 10 min of curing; (c) after 20 min of curing; (d) after 30 min of curing.

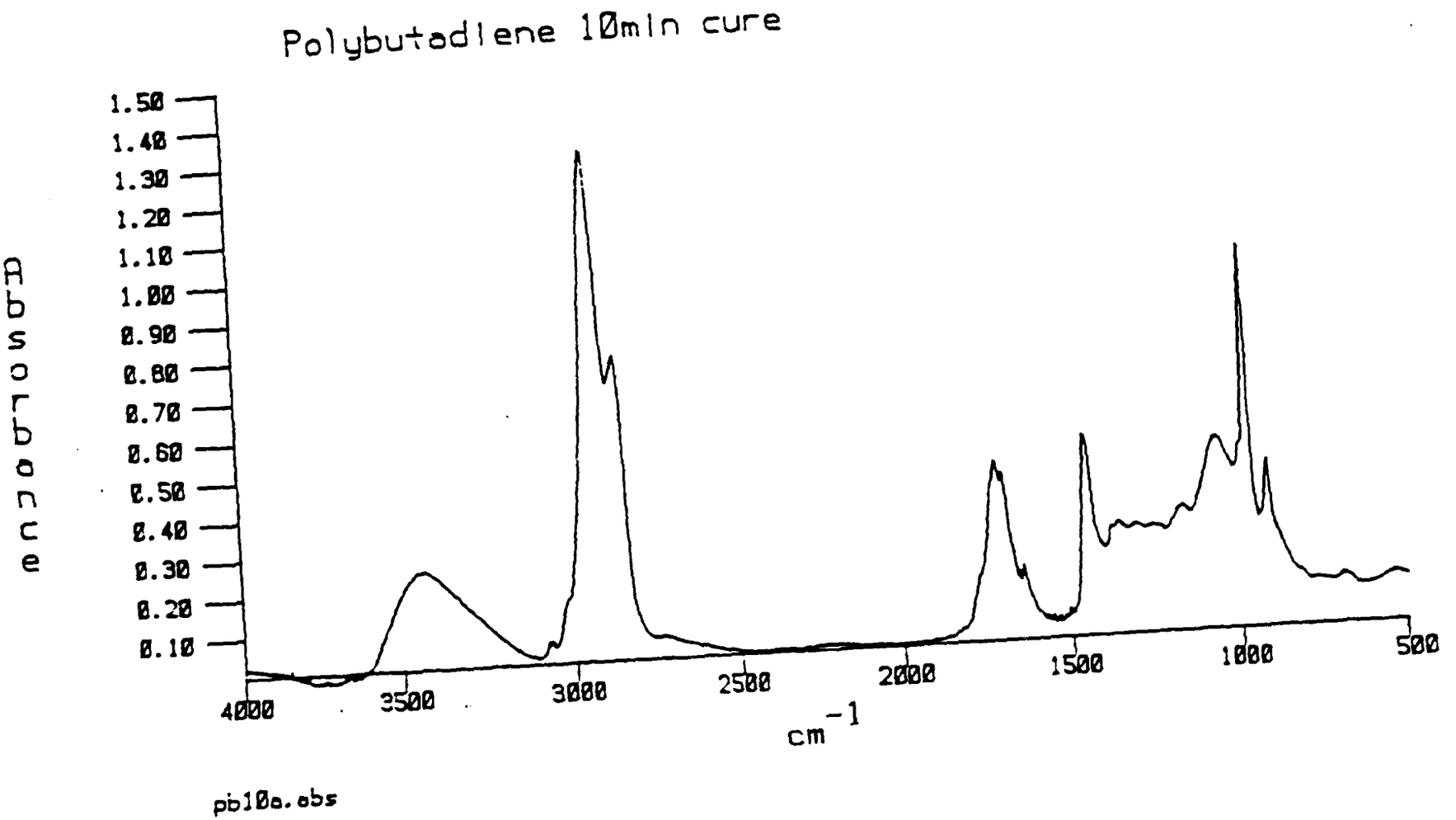

Figure 7(b). (Cont'd.)

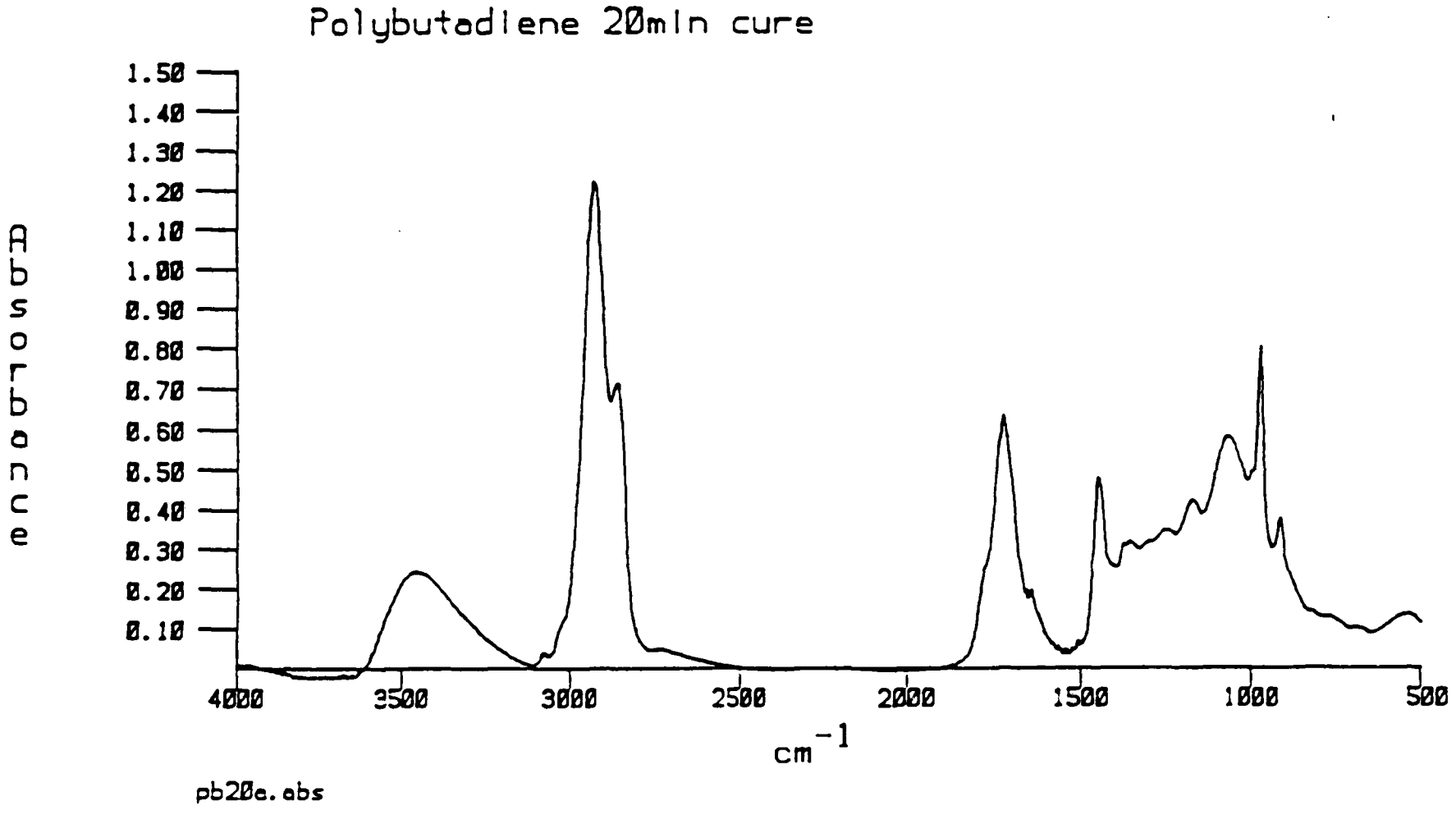

Figure 7(c). (Cont'd.)

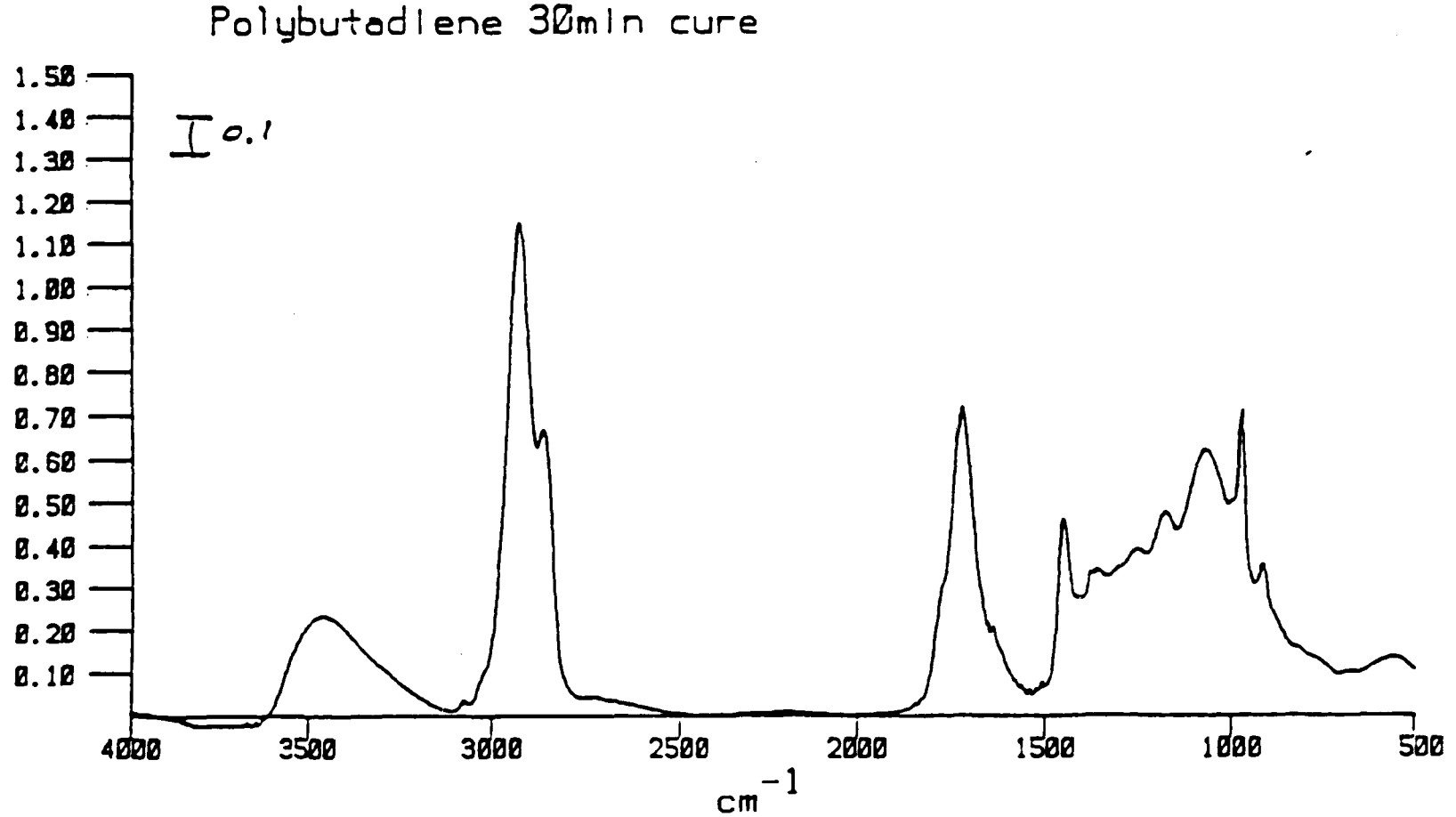

Figure 7(d). (Cont'd.)

neighbor environment. One of the early experiments done to test its applicability to this problem will now be described [17].

Sodium ions were introduced into polybutadiene coatings on steel by the application of a cathodic potential. The subsequent delamination that occurred permitted the removal of the coating from the metal, thorough washing in water and insertion of sufficient coating into the spectrometer cavity to develop a satisfactory NMR spectrum. A representative spectrum is shown in Figure 8 in which it can be seen that there exists a sharp peak superimposed on a broad background absorption peak. Our preliminary interpretation of this experiment is that the sharp peak represents the sodium ion in an aqueous phase within the easy charge transport pathways, and the broad peak represents the sodium ion present in the polymer matrix in a very large number of slightly different chemical environments. This preliminary interpretation is supported by the observation that the sharp peak disappears when the coating is dried, as shown by the spectrum in Figure 9. The spectrum shown in Figure 8 was regenerated when the dried sample was exposed to water.

An important aspect of the morphology of coatings is the effect of pigments and fillers. It is well known that some pigments and fillers develop strong interactions with the polymer matrix while others do not. The ability of aqueous pathways to form adjacent to the pigments and fillers is determined to an important extent by the type of interaction between the pigment or filler and the polymer matrix. Our research in this subject area is limited at the present time.

A second approach to an understanding of the morphology of coatings utilizes positron annihilation. When positrons are implanted in polymeric coatings, their lifetimes fall in three different ranges, a short lifetime of the order of 200 ps, an intermediate lifetime of the order of 500 ps and a long lifetime of the order of 2500 ps. The physical processes that are reponsible for the two shorter lifetimes in polymeric materials are not firmly established but the long lifetime is associated with the formation of orthopositronium within voids in the polymer matrix. The size of these voids has not been determined but we are conjecturing that they have dimensions of 1 nm or more. Recently, the positron annihilation spectra have been determined for 4 epoxy coatings and a vinyl ester coating. The percentage of positrons annihilated with the long lifetime are summarized in Table IV. It will be noted that the solvent-based coatings that were cured at room temperature had values for the long-lifetime intensity in the range of 15-21% whereas the corresponding value for the powder coating which was cured at 200°C was 11%. Since the chemical natures of the epoxy coatings are all very similar, it is concluded that the low value in the case of the material cured at 200°C is a consequence of the absence of solvent and the formation of a coating that has a minimum number of voids. Solvent-based coatings presumably leave residual voids during the drying process when the coating begins to become firm and solvent is still exiting the coating.

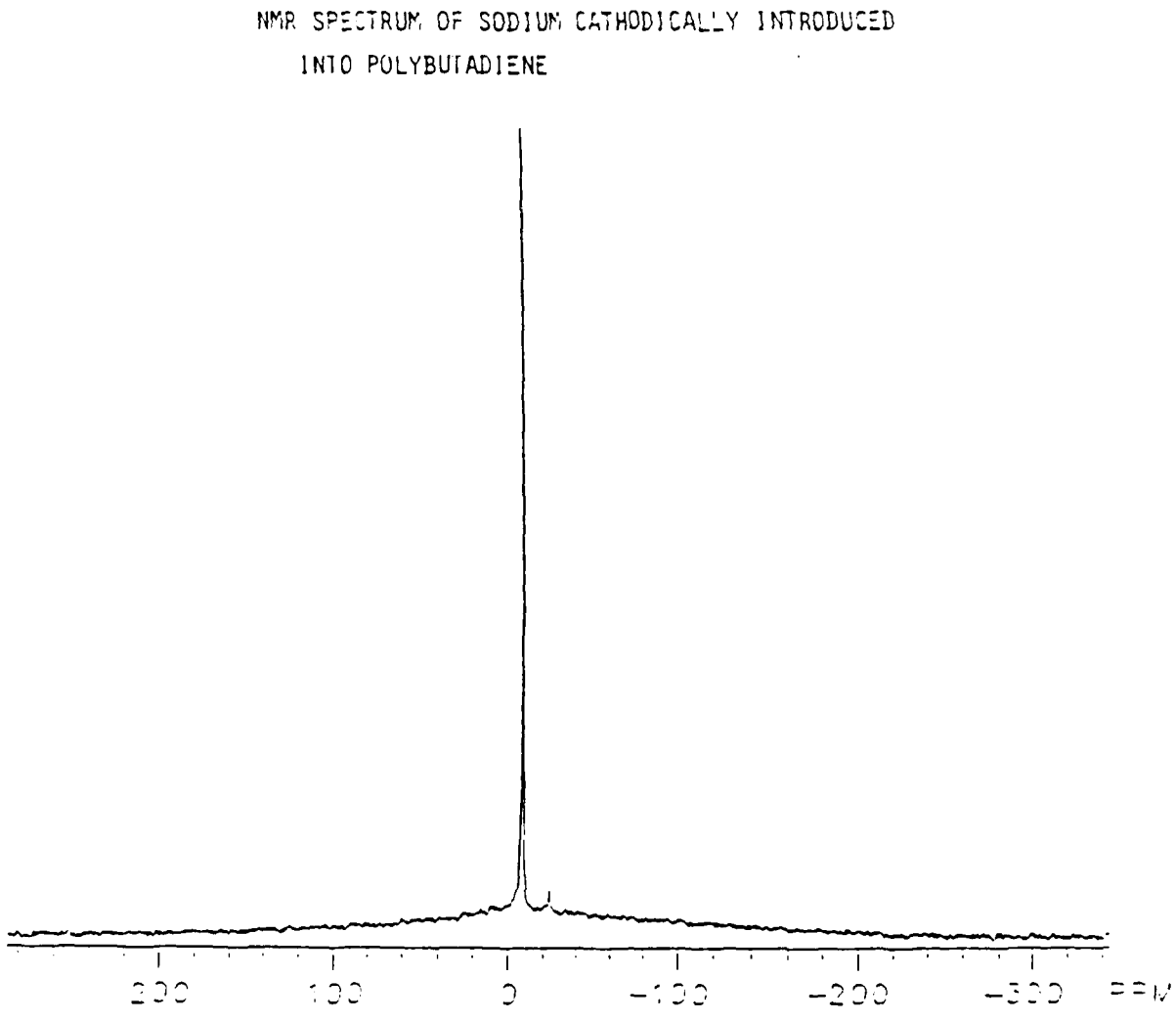

Figure 8. NMR of Na^+ introduced into a polybutadiene coating on steel by the application of a cathodic potential while exposed to 0.5M NaCl [17]. Data are given with reference to solid NaCl.

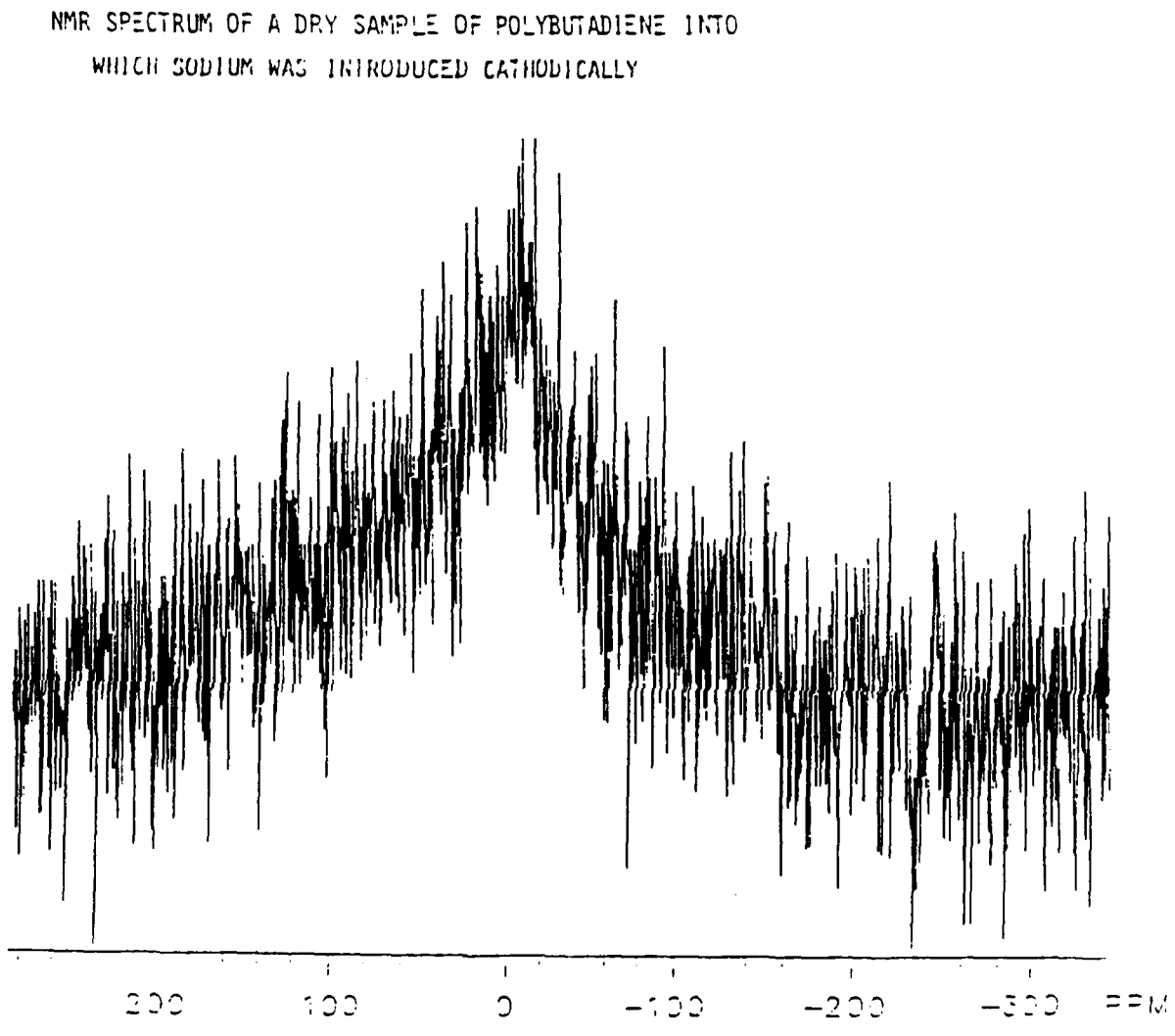

Figure 9. NMR spectrum of Na^+ introduced into a polybutadiene coating on steel by the application of a cathodic potential while exposed to 0.5M NaBr. Coating was dried before the spectrum was determined [17]. Data are given with reference to solid NaCl.

Table IV

Positron Annihilation Behavior in Five Coatings

Type of Coating	% of Positrons Annihilated in Large Voids
Powder epoxy	11.2%
Vinyl ester (solvent)	17.4
Epoxy #2 (solvent)	20.7
Epoxy #3 (solvent)	15.2
Epoxy #4 (solvent)	16.7

The presence of solvent in aggregated form within the coating is suggested by the fact that hydrophilic solvents remaining in the coating cause blisters to form when the coating is exposed to pure water at elevated temperature. Activity gradients between water and solvent in the polymer matrix and that between the solvent/water mixture in a liquid phase within the matrix cause the liquid phase to increase in volume locally within the coating and the coating to blister consequently.

Impedance measurements of coatings cured at different temperatures also provide useful information. Table V provides data on the impedance of 6 different coating systems, 3 cured at elevated temperature and 3 cured at room temperature. The coatings cured at the elevated temperature exhibited impedances at low frequency in the range of 10^{11} to 10^{12} ohm·cm^2 whereas the coatings cured at room temperature had impedances of 10^6 to 10^8 ohm·cm^2. Our interpretation of these representative data is that the high temperature curing removed the pathways which are the origin of the charge pathways responsible for the low impedance values.

There is substantial evidence that the exterior portion of the coating cures at room temperature at a faster rate than the interior of the coating and especially than at the metal interface. This cured "surface skin" reduces the rate of solvent evaporation and probably plays an important role in determining the eventual morphology of the coating. The long-term entrapment of solvent is important in determining the physical characteristics of the coating upon aging.

Table V
Data Showing the Importance of Curing Temperature on the Impedance at Low Frequency of Coatings on Steel

Type of Coating	Temp. of Cure	Thickness (μm)	Log Impedance at 10^{-3}Hz* (ohm·cm^2)
Baked polyester	200°C	30	11
Epoxy powder	180	100	12
Polybutadiene (some sections)	200	25	11
Acrylic-urethane	RT	60	8
Epoxy solvent	RT	210	8
Alkyd	RT	100	6

* - after exposure to 0.5M NaCl for 1 day

CHEMICAL NATURE OF AN ION IN A COATING

As stated previously, it has been shown that the rate of cathodic delamination of coatings on steel is determined by the rate of transport of the cation through the coating. It has also been shown in published [2,18] as well as unpublished work that the cathodic delamination in alkali chloride solutions increases in the order Li^+, Na^+, K^+, Cs^+. An example is shown in Figure 10. This order has been observed in all coating systems studied including polybutadiene, epoxy, alkyd and acrylic coatings. A similar order has been observed in cathodic blistering studies of an epoxy primer coating on steel [19]. This order parallels the size of the ion including its hydration sheath. The size of the hydrated ion is reflected in the transference number of the cation and the diffusion coefficient which all increase in the order: Li^+, Na^+, K^+, Cs^+. This correlation strongly suggests that the nature of the cation in these polymer matrices is the hydrated species. The ions thus do not lose their hydration sheath when they leave the electrolyte and enter the polymer matrix. Since the water molecules surrounding the cation are held there by electrostatic forces, it is likely that this sheath is readily deformed as the ion takes its random walk through the polymer.

Another approach to understanding the nature of an ion in a polymer matrix is based on emission Mössbauer spectroscopy. Mössbauer-active ions such as ^{57}Co and ^{129m}Sn were introduced into alkyd, epoxy and polybutadiene coatings and the gamma ray spectrum of the ion in the matrix was determined [20,21]. In the case of Co^{+2} it was possible to implant the ion only in the alkyd coating whereas it was possible to implant the Sn^{+4} ion into all three

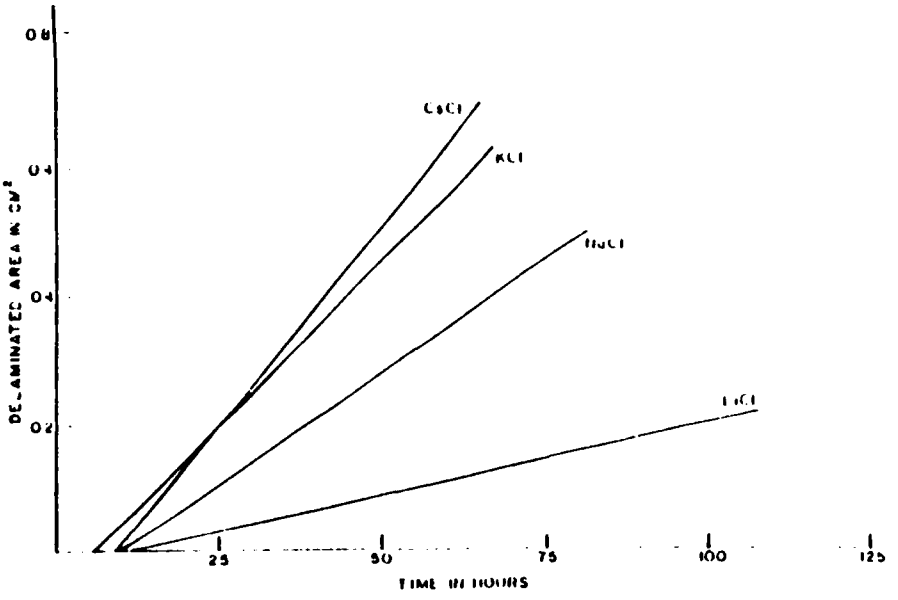

Figure 10. The relative rates of the cathodic delamination of polybutadiene from steel when polarized at -0.8 V vs. SCE in different 0.5M alkali halide solutions.

coatings. On the basis of the emission spectrum, the cobalt ion was interpreted to be associated with carboxylate ions within the coating. The tin ion, on the other hand, existed in the coating as an isolated ion in a symmetrical chemical environment and with an ionicity greater than the tin atom in tin dioxide.

Studies have been initiated seeking to determine if ^{13}C NMR spectroscopy can be used to obtain a better understanding of Na^+ ions present in a coating. Preliminary experiments have shown differences in the spectrum before and after introduction of sodium into a coating. It is not known at the time of writing whether these changes in the spectrum are a consequence of the introduction of the Na^+ ion or arise from another source.

SUMMARY

The studies discussed here further support the conclusion that the cation transport through protective polymeric coatings exposed to an aqueous electrolyte occurs largely by means of aqueous pathways. The major fraction of cations in a coating exist within these pathways.

ACKNOWLEDGEMENT

It has been our privilege to cooperate with Don Seraphim and his colleagues at IBM-Endicott on technical issues related to photoresists and corrosion protective coatings. It is an honor to be part of the group acknowledging his contributions to technology. Appreciation is expressed to the Office of Naval Research who provided support for much of the research described herein. Special appreciation is expressed to the following colleagues for the privilege of citing unpublished data: J. Roberts, R. Turoscy, A. Vértes and P. Deck.

REFERENCES

[1] H. Leidheiser, Jr., and W. Funke, J. Oil Colour Chem. Assoc. 70(5), 121 (1987).

[2] H. Leidheiser, Jr., J. Adhesion Sci. Tech. 1, 79 (1987).

[3] "Ions in Polymers," A. Eisenberg, Ed., Adv. Chem. Series 187, Am. Chem. Soc., Washington, D.C., 1980, 376 pp.

[4] R. C. Bacon, J. J. Smith and F. M. Rugg, Ind. Eng. Chem. 40, 161 (1948).

[5] H. Leidheiser, Jr., Prog. Org. Coatings 7, 79 (1979).

[6] H. Leidheiser, Jr., R. D. Granata, and R. Turoscy, Corrosion 43, 296 (1987).

[7] J. E. O. Mayne and D. J. Mills, J. Oil Colour Chem. Assoc. 58, 155 (1975).

[8] H. Leidheiser, Jr., D. J. Mills and W. Bilder, Proc. Symp. Corrosion Protection by Organic Coatings, M. W. Kendig and H. Leidheiser, Jr., Eds., Electrochem. Soc. Vol. 87-2, 1987, pp. 23-36. (This paper was originally presented at the 1986 Fall meeting of The Electrochemical Society, Inc., held in San Diego, CA.)

[9] H. Leidheiser, Jr., M. W. White and D. J. Mills, Elec. Power Res. Inst. Report CS-5449, October 1987, 103 pp.

[10] H. Leidheiser, Jr., M. De Crosta and R. D. Granata, Corrosion 43, 382 (1987).

[11] F. Mansfeld and M. W. Kendig, Corrosion 41, 490 (1985).

[12] S. Haruyama, M. Asari and T. Tsuru, Proc. Symp. Corrosion Protection by Organic Coatings, M. W. Kendig and H. Leidheiser, Jr., Eds., Electrochem. Soc. Vol. 87-2, 1987, pp. 197-207.

[13] H. Leidheiser, Jr., M. L. White, R. D. Granata and H. L. Vedage, Elec. Power Res. Inst. Report CS-4546, May 1986, 102 pp.

[14] J. Parks and H. Leidheiser, Jr., Ind. Eng. Chem. Prod. Res. Dev. 25, 1 (1986).

[15] H. Leidheiser, Jr., and M. W. Kendig, Corrosion 32, 69 (1976).

[16] P. Deck, Ph.D. Thesis Research, Lehigh University, 1987.

[17] J. Roberts, R. Turoscy and H. Leidheiser, Jr., work in progress.

[18] J. M. Atkinson, R. D. Granata, H. Leidheiser, Jr., and D. G. McBride, IBM J. Res. Dev. 29(1), 27 (1985).

[19] V. Rodriguez and H. Leidheiser, Jr., to appear in J. Coatings Technol.,

Feb. 1988.

[20] H. Leidheiser, Jr., A. Vértes, I. Czakó-Nagy and M. Farkas, J. Electrochem. Soc. 134, 823 (1987).

[21] H. Leidheiser, Jr., I. Czakó-Nagy and A. Vértes, J. Electrochem. Soc. 134, 1470 (1987).

EMISSION MÖSSBAUER STUDIES OF THE COBALT/ORGANIC COATING INTERFACE

Philip Deck and Henry Leidheiser, Jr.

This paper will be presented at a meeting of the American Chemical Society to be held in Toronto, June 5-10, 1988

EMISSION MÖSSBAUER STUDIES OF THE COBALT/ORGANIC COATING INTERFACE

Abstract

A thin electrodeposit containing ^{57}Co was electrodeposited on cobalt metal sheet. Organic coatings of both air-dry and baked type were applied. Changes in the spectrum were interpreted on the basis of chemical interactions at the interface. In some systems, minimal changes in the spectrum were detected before and after the application of the coating. In other systems, substantial changes occurred immediately after baking or, in the case of air-dry systems, after storage at room temperature for several months.

INTRODUCTION

Coatings are applied to metals to provide the substrate metal with protection from the environment and, hence, retard the onset of corrosion. The protection the coating provides is, in a large way, determined by the integrity of the interface between polymer and metal. The study of this interfacial region is hindered by the difficulty in probe access to the interface. Some studies have provided information on failure mechanisms of the interface by studying the surface chemistries of the cleaved interface [1]. The goal of our research is to understand the chemistry of the intact interface and the interactions occurring between polymer and oxidized surface of the metal.

Emission Mössbauer spectroscopy has been shown to be a useful technique for the evaluation of surface cobalt species [2]. Further, a preliminary emission Mössbauer study of an oxidatively cured polybutadiene resin on a radioactive cobalt substrate [3] has given evidence of Co(III) to Co(II) reduction indicative of the interaction between polymer and metal oxide phases across the interface.

Electrodeposition of less than a monolayer of ^{57}Co onto a cobalt substrate yields a surface-sensitive Mössbauer-active source. Spectra recorded prior to and after polymer coating provide insight into chemical changes occurring at the cobalt/polymer interface.

EXPERIMENTAL

Cobalt foil, 0.25 or 0.50 mm thick and of 99.9965% purity, served as the substrate for the electrodeposited radioactive cobalt. The foil was cut into 25 x 25 mm squares and polished using standard metallographic techniques. The foils were degreased with trichloroethylene prior to etching in a 50:50 H_2SO_4:HNO_3 solution. The etched foils were rinsed in distilled water and methanol, and stored in a desiccator prior to electrodeposition. Immediately prior to electrodeposition, the foils were swabbed with trichloroethylene.

The electrodeposition procedure was that used by Deszi and Molnar [4]. The stock solution consisted of 0.25 g/ℓ ammonium citrate and 0.25 g/ℓ hydrazine hydrate adjusted to a pH greater than 10 using ammonium hydroxide. To 5 ml of this stock solution were added 1 mCi of ^{57}Co as carrier-free cobaltous chloride in 0.5N HCl obtained from Dupont New England Nuclear. After addition of the ^{57}Co to the stock solution, the pH was checked and adjusted if necessary. It was found that 4 specimens could be prepared from a solution of 1 mCi initial activity.

A current density of 1.6 mA/cm² flowed through the solution between the cobalt cathode and a platinum grid anode. Deposition times ranged from 3 to 8 h depending on the solution activity. After deposition, the cobalt foil was carefully rinsed with distilled water and allowed to air dry. Activities for the deposited foils were on the order of 10^7 Bq, which for ^{57}Co with a half life of 270 d, represents a deposit of 10^{-5} mg or an average coverage of less than a monolayer of ^{57}Co over the 227 mm² deposited area.

Auger electron spectroscopy of the electrodeposited cobalt confirmed the presence of cobalt as the only metallic element and scanning electron microscopy revealed an island-like morphology of the deposit.

Table 1 lists the polymers studied using this technique. The polymers or their solution were smeared or spin-coated onto the cobalt foil and allowed to air-dry or were baked as prescribed in Table 1. Coating thicknesses exceeded 20 μm.

A schematic diagram for the emission Mössbauer experiment is shown in Fig. 1. the electrodeposited cobalt substrate serves as the gamma ray source and an ^{57}Fe enriched stainless steel foil serves as the absorber. Data acquisition times ranged from 25 to 168 h. Mössbauer spectra were recorded at room temperature for each foil as deposited and after coating application and cure.

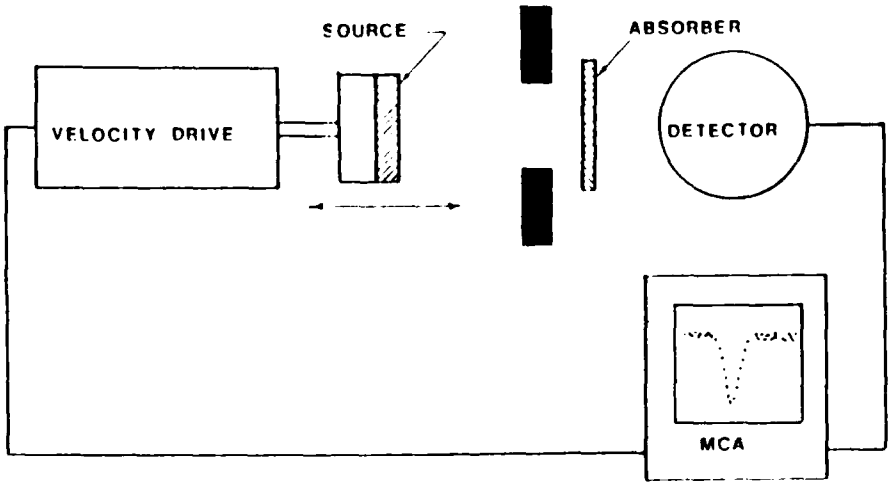

Fig. 1. Schematic profile for the Mössbauer experiment. In an emission experiment, the ^{57}Co electrodeposited foil serves as the source of gamma-rays. An ^{57}Fe enriched stainless steel foil served as the absorber.

The velocity and zero velocity channel were calibrated periodically using ^{57}Co in platinum as the source and an ^{57}Fe foil absorber. The spectra were folded and fitted using a linear combination of Lorentzian and Gaussian peak shapes in a sextet fitting subroutine of the SIRIUS Evaluating System [5] on a Cyber 730 computer. Isomer shift values are reported relative to α-iron.

Table 1

POLYMER COATINGS

Coating	Description	Solvent	Trade Name	Cure
polybutadiene	60% trans 1,4 19% cis 1,4 21% vinyl 1,2	petroleum distillates	DuPont RKY Budium basecoat	30 min @190°C
poly(amic acid)	condensation product of 4,4 oxydianiline and 1,2,3,5 benzene tetracarboxylic anhydride	N-methyl 2-pyrrolidone and xylene	DuPont Pyre-ML wire enamel	12 min @85°C
polyimide	condensation product of poly(amic acid)	see poly(amic acid)		20 min @200°C
thermoplastic polyimide		N-methyl 2-pyrrolidone	M&T 5000 thermoplastic polyimide	1 h @100 1 h @200
poly(acrylic acid)		methanol	Aldrich	air-dry
polyacrylamide		water	Aldrich	air-dry
silicone alkyd	silicone modified medium/long oil alkyd	VM&P naphtha, toluene, isobutyl isobutyrate	McCloskey Varkyd 385-50E	air-dry
acrylic	PMMA acrylic	toluene	Rohm & Haas Acryloid B-66	air-dry
vinyl ester	vinyl ester with DMA N,N dimethyl aniline, Co naphthalene, and MEK peroxide		Dow Derakane 8084	air-dry
epoxy	bisphenol A hardened with aliphatic amine		Ciba-Geigy Araldite CG 2600 resin & H9943 amine hardener	air-dry

RESULTS AND DISCUSSION

Figure 2 shows the Mössbauer spectra obtained for a ^{57}Co electrodeposit prior to and after poly(acrylic acid) (PAC) application. The spectrum for the as-deposited cobalt reveals that almost 80% of the radioactive cobalt is in a metallic state. Roughly 20% of the deposit is present as CoOOH [6] and $Co(OH)_2$ makes up the remainder. After PAC application, the metallic cobalt component of the spectrum is no longer observed and the Co(II) component greatly increased in intensity. The hyperfine parameters measured for this component identify it most closely as a Co(II) carboxylate [7,8]. Hence, the metallic cobalt at the interface reacts with the acid groups of PAC. A similar phenomenon has been recorded for poly(amic acid) applied to cobalt, even after thermal cure to polyimide [9].

The result of coating application of polyacrylamide (PAM) applied to cobalt (see Fig. 3) is again striking. Much of the metallic cobalt is no longer observed in the spectrum after PAM application. Instead of an increase in Co(II) fraction as was observed for PAC, it is the Co(III) component that increases. Because the PAM was applied as an aqueous solution, it is believed that the water promoted the oxidation of the metallic cobalt to CoOOH.

Oxidation of the cobalt substrate is observed for an uncoated electrodeposited sample after several months' storage in a desiccator. However, the degree of oxidation is slight in comparison to that observed for the PAM-coated sample. A thermoplastic-acrylic-resin-coated cobalt substrate exhibited about the same degree of oxidation after 3 months as did the bare cobalt, indicative of this coating's lack of any strong interaction with the substrate cobalt.

Other commercial coatings showed a range of behaviors. The application of both an amine hardened epoxy and a vinyl ester resulted in increases in the fraction of Co(II) in the spectra. The vinyl ester coating spectrum also exhibited a small drop in the quadrupole splitting value of the Co(II) fraction, a fact which may be indicative of carboxylate formation.

A silicone-modified alkyd showed no immediate spectral changes, but after 3 months' aging, exhibited a reduction of Co(III) to Co(II) as had been shown for polybutadiene [3]. Both polybutadiene and the alkyd cure via oxidative mechanisms, although polybutadiene oxidizes relatively quickly by thermal treatment, while the alkyd oxidizes more slowly at room temperature.

SUMMARY

The chemistry of the interfacial oxide is dependent on the nature of the film formation properties, functional groups, and solvent of the coating. For polymers undergoing oxidation, the cobalt oxide participates in the oxidation as evidenced by a reduction of its Co(III) oxide. Pendant functional groups, such as acids, and perhaps esters, may react with the cobalt substrate, to form carboxylate bonds. Coatings which are water-based may promote oxide formation at the interface.

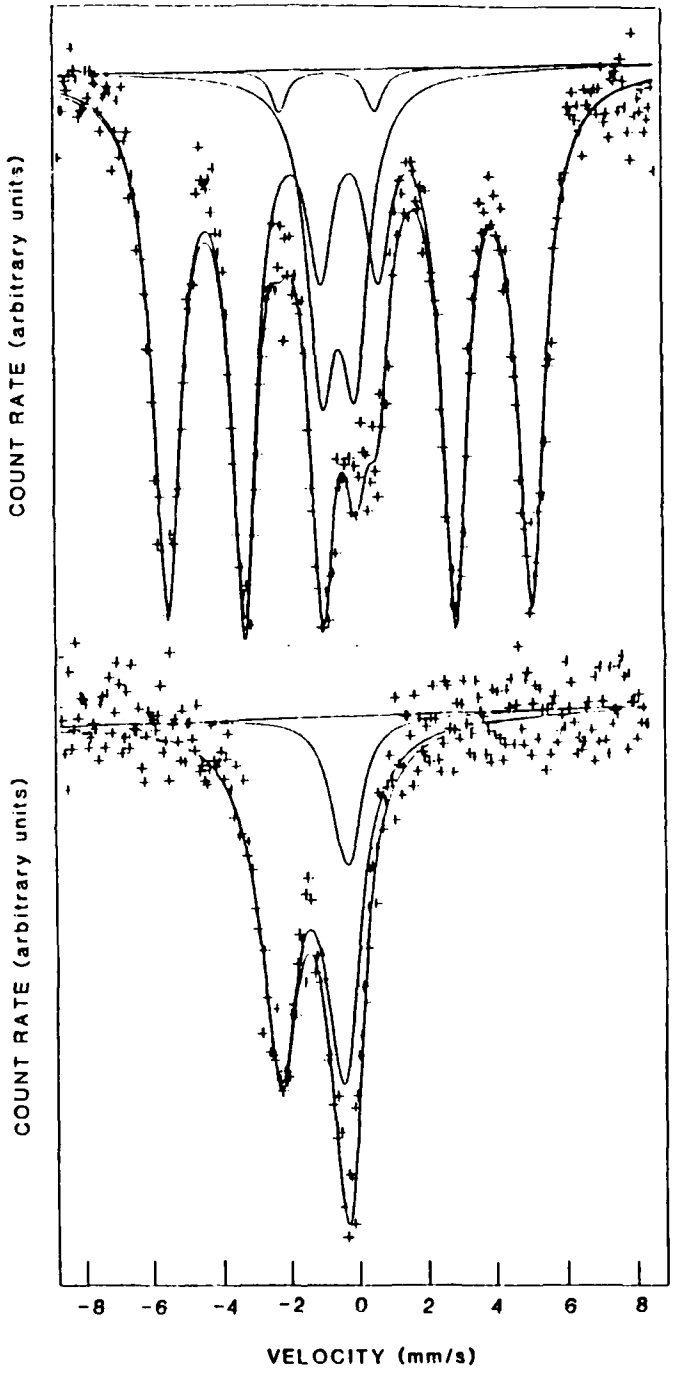

Fig. 2. ^{57}Co emission Mössbauer spectrum obtained for an electrodeposited cobalt foil (top) prior to coating application, and (bottom) after application of a poly-(acrylic acid) solution.

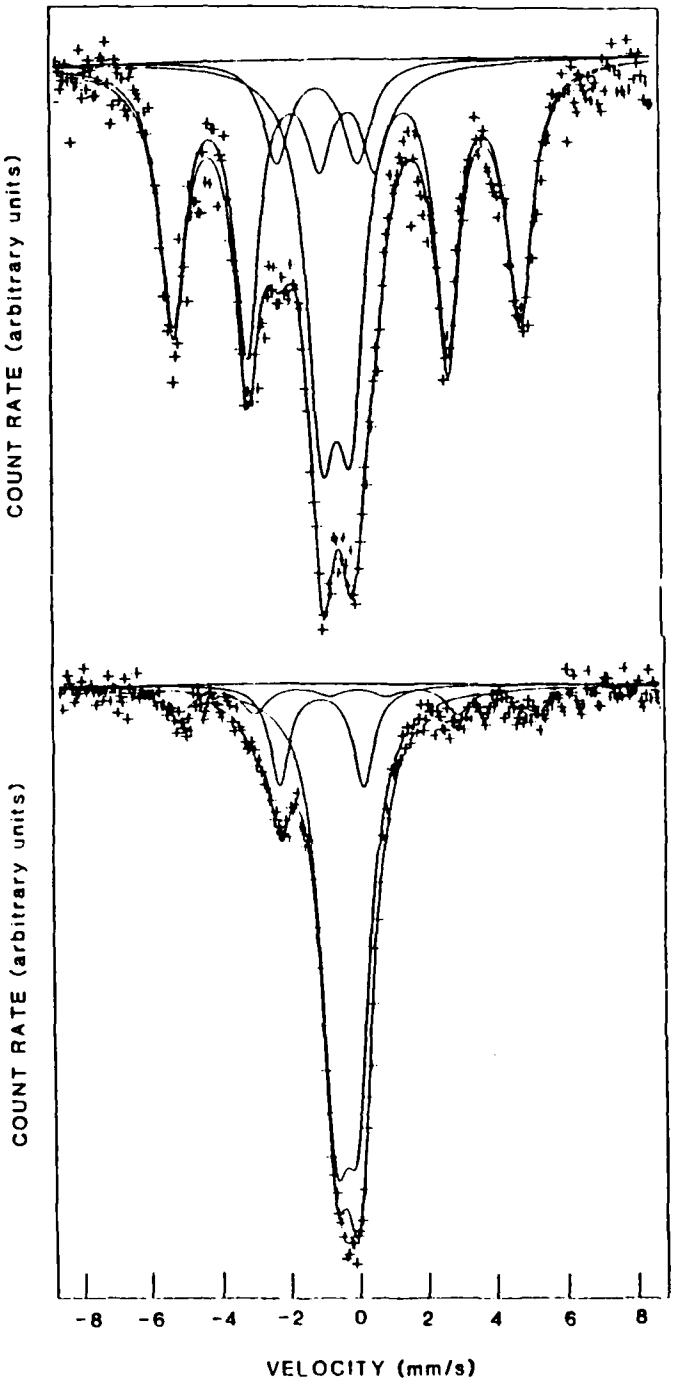

Fig. 3. ^{57}Co emission Mössbauer spectrum obtained for an electrodeposited cobalt foil (top) prior to coating application, and (bottom) after application of a polyacrylamide solution.

REFERENCES

[1] J.S. Hammond, J.W. Holubka, J.E. deVries, and R.A. Dickie, Corrosion Science 21 (1981) 239.
J.E. Castle and J.F. Watts, Ind. Eng. Chem. Prod. Res. Dev. 24 (1985) 361.
J.F. Watts and J.E. Castle, J. Materials Sci. 19 (1984) 2259.

[2] G.W. Simmons, E. Kellerman, H. Leidheiser, Jr., J. Electrochem. Soc. 123 (1976) 1276.

[3] H. Leidheiser, Jr., S. Music, and G.W. Simmons, Nature 279 (1982) 667.

[4] I. Deszi and B. Molnar, Nucl. Inst. Methods 54 (1967) 105.

[5] S.I. Nagy and T.W. Weir, SIRIUS Spectrum Evaluating System, Lehigh University.

[6] G.W. Simmons in "Passivity of Metals," R.P. Frankenthal and J. Kruger, Eds., The Electrochemical Society: Princeton, NJ, 1978, pp.898-917.

[7] J.M. Friedt and L. Asch, Radiochimica Acta 12 (1969) 208.

[8] R.W. Grant et al., J. Chem. Phys. 45 (1966) 1015.

[9] A. Vértes, I. Czakó-Nagy, P.D. Deck, H. Leidheiser, Jr., J. Electrochem. Soc. 134 (1987) 1628.

POSITRON IMPLANTATION AND ANNIHILATION IN PROTECTIVE ORGANIC COATINGS

Cs. Szeles, K. Süvegh, A. Vértes, M. L. White and H. Leidheiser, Jr.

This paper has been accepted for publication in the
JOURNAL OF COATINGS TECHNOLOGY

Positron Implantation and Annihilation in Protective Organic Coatings

ABSTRACT

Positron implantation and annihilation were studied in two polymeric coatings, one pigmented and the other unpigmented, deposited on steel substrates. Positron lifetime spectra recorded on the coatings exhibited three components and closely resembled characteristic lifetime spectra of bulk polymers, but they were strongly dependent on the coating thickness. It was shown that the lifetime spectra could well be described as a sum of two contributions: spectra of the coating and the steel substrate. The fraction of positrons stopped in the coatings and in the steel were determined, and the effective mass absorption coefficients of positrons were extracted. The thickness dependence of the mean positron lifetime and the intensities of different lifetime components were described with an exponential positron implantation profile. The mixing of the lifetime parameters of the coating and steel spectra was studied as a function of thickness. Simulated lifetime spectra were generated using the experimental lifetime spectra and implanted fractions in the coatings and steel. Differences between the measured and simulated lifetimes and intensities at low thickness values were associated with an inhomogeneous size and depth distribution of open volumes in the coatings.

INTRODUCTION

Protection of metal surfaces from corrosion is among the more important applications of organic coatings. Five major subject areas in which many questions relative to corrosion protection are unanswered have been described in a recent publication [1]. One of these subject areas relates to the size and number of voids present at the metal/organic coating interface. Means for determining the presence of these voids are not obvious because optical measurements are impractical with opaque coatings. Recent success [2-4] in the application of positron annihilation to the study of protective organic coatings led us to initiate research on the use of this technique for studying voids in organic coatings since positron annihilation is sensitive to vacancies and voids in solid materials.

Experimental methods based on the annihilation properties of positrons injected into materials have been widely used to study open volume defects in a range of materials [5,6]. It has also been successfully applied to study the structure of molecular materials and the structural changes that occur upon phase transitions, ion uptake, radiation damage, etc. [7]. New experimental methods based on controlled energy, monoenergetic positron beams have now been developed for the study of surfaces and interfacial phenomena [8,9]. These methods hold great promise for the study of the interface between thin organic coatings and a metal, but they do not appear applicable to the study of protective organic coatings whose thickness is in the 25-600 μm range. The more conventional methods for studying positron annihilation appear to have more promise in the area of our present interest [2-4,10,11].

Positrons, when injected into a solid, tend to be localized at regions of lower than average ionic charge density. Since the electron distribution and the density are different at such sites, the annihilation properties of the positrons may be completely different in these trapped states. The annihilation probability of the trapped positron depends largely on the average electron density in the free volume and it is thus sensitive to both the volume and geometry of the free volumes. If the size of the free volume is large and consequently the electron density therein is low, positronium formation and localization may take place within these free voids. The chemical nature of the boundaries of the free volumes influences the positronium lifetime since the annihilation properties of the positronium atoms, as well as the electron density, are sensitive to the polarization effects of atoms at the boundary. Experimental methods based on positron annihilation are particularly fruitful when relatively small changes in the ionic or electronic structure of free volumes and their surroundings are studied.

Recently we have studied the positron annihilation properties in protective organic coatings before, after and during exposure of the coated metal to water [2-3]. The ability to draw correlations between the positron lifetimes and the protective properties of the coatings in an aggressive environment encouraged us to pursue this work further. An important shortcoming of the prior work was the poor knowledge of the depth distribution of positrons in the metal/coating system. The reported lifetime spectra represented the sum of the lifetime distributions in the coating and in the metal, weighted by the fraction of positrons stopped in the two layers. Therefore, in order to interpret lifetime spectra recorded on protective coatings, it is essential to know the positron stopping profile in the metal/coating system.

The work reported herein was designed to clarify the role of different contributions to the measured lifetime spectra, to advance the analysis of such spectra, and to gain additional insight useful in interpreting the spectra. To achieve these goals we have determined the effective mass absorption coefficients and implantation profiles of positrons in two coatings, one a fully formulated, commercial system and the other a neat resin system without pigments or fillers. The major parameter that was varied was the coating thickness. The thickness dependence of the positron lifetime spectrum parameters was studied on computer-generated spectra. These were obtained using the experimental fractions of positrons stopped in the coatings and in the metal. It will be shown in the discussion that follows that differences in the measured and calculated spectra may be accounted for by a change in the defect structure in the vicinity of the metal/coating interface.

EXPERIMENTAL

The alkyd based coating was a formulated, commercial material (Rust-Oleum Flat White #7790). It was applied as received to discs of cold-rolled steel 1-5/16 inch (3.3 cm) in diameter and 32 mils (0.80 mm) thick by spinning at 1000 rpm. Sample thicknesses between 3 mils (0.08 mm) and 23 mils (0.58 mm) were obtained by multiple spinning, with a 45 min air dry between coats and a final bake at 60°C for about 1 h.

The epoxy coating was a novolac resin cured with a mixed aromatic/aliphatic amine (2:1 ratio, by weight) obtained from Ciba-Geigy Corporation. The mixed resin/hardener material was applied to cold rolled steel by a draw down procedure, using an adjustable Gardner knife. The thickness varied from 2.5 mils (0.063 mm) to 17.7 mils (0.44 mm). Curing was done at room temperature. The coated steel was then cut into 1-1/2 inch (3.8 cm) squares. The surface finish on the steel substrates for both coatings was 35-50 microinches (0.89-1.27 μm).

The lifetime spectrometer was a conventional fast-slow coincidence system based on NE 111 plastic scintillators, XP 1021 photomultipliers and ORTEC electronics. The time-resolution of the system was around 300 ps full width at half maximum. In most cases, it was reliably described with a single or eventually two Gaussians. The positron source was made by deposition of carrier-free $^{22}NaCl$ solution between 1 mg/cm^2 thin Kapton foils. The lifetime spectra were measured at room temperature and normal pressure, and were collected within one day. The **RESOLUTION** and **POSITRONFIT** computer programs were used [12] to evaluate the lifetime spectra. The spectra were fitted with three components which are described in terms of the lifetime (τ) and the intensity (I).

There are several experimental methods to determine positron depth distribution in a given material [13,14]. Here we have applied the method developed in the 1960's [15,16], which uses a simple sandwich geometry and is based on the large differences between the lifetime spectra of polymers and steel (see Table 1). The measured spectra were assumed to be linear superpositions of these two contributions weighted by the relative fraction of positrons stopped in the two materials. The positron implantation profile and effective mass absorption coefficients were determined from positron lifetime spectra on coatings of increasing thickness.

RESULTS

Lifetime spectra of the coatings and the steel substrate are given in Table 1. The coatings data were obtained from spectra recorded on the thickest alkyd coating, as this coating absorbed almost all the injected positrons, and on a stack of detached epoxy coatings of total thickness about 1800 μm.

Table 1. Lifetime spectra of the coatings and the cold-rolled steel substrate*

Material	τ_1 (ps)	τ_2 (ps)	τ_3 (ps)	I_1 (%)	I_2 (%)	I_3 (%)
Alkyd	178±3	480±8	2520±30	48.8±1.3	42.5±1.3	8.8±0.2
Epoxy	188±4	520±20	1830±23	43.7±1.6	34.0±1.3	22.3±0.5
Steel	136±3	276±10	--	78.0±1.0	22.0±1.0	

Figure 1 shows the mean positron lifetimes, while Figures 2 and 3 show extracted lifetimes and intensities versus coating thickness for the alkyd and epoxy, respectively. The lifetime parameters show the expected saturation behavior. Spectra converge toward the spectra of the coatings with increasing coating thickness due to an increased positron absorption in the coatings and a decreased fraction of positrons reaching the metal.

Three major differences in the spectral features of the two coatings may be noted.

(i) There is a striking difference between the long-lived components. The epoxy coating exhibits a much higher intensity and shorter lifetime for this component.

(ii) Saturation of the parameters takes place at a much lower thickness value in the case of the alkyd coating because of its higher density.

(iii) The value for the long lifetime increases considerably with increasing thickness for the alkyd coating while it is almost constant in the case of the epoxy coating.

---

*Data given in the table are somewhat different from results published earlier [4]. The differences are due to a more precise treatment of the resolution function and more consistent analysis of the steel spectra in terms of two lifetime parameters. The statistically most reliable parameters, mean lifetimes and I_3 are not appreciably influenced by the differences in the data treatment.

DISCUSSION

Positron Implantation

The lifetime parameters depicted in Figures 1-3 tend towards saturation above 300 μm and 600 μm in the case of alkyd and epoxy, respectively. This is most clearly seen in the behavior of the mean positron lifetime (Fig. 1) which is the most statistically reliable parameter. As the density of the pigmented alkyd coating, $\delta = 2.03$ g/cm^3 is almost a factor of two higher than the density of the unpigmented epoxy coating, $\delta = 1.13$ g/cm^3, the above thickness values roughly correspond to 60 mg/cm^2 reduced thickness value in both cases. Below this value, the thickness of the coatings is insufficient to stop all the positrons and a fraction of the positrons traverses the coating and reaches the metal. Any lifetime spectrum below this coating thickness contains a significant contribution from positrons decaying in the steel beneath the coating. The measured lifetime spectra are then summations of the spectra of the coating and the steel.

The large differences between the lifetime spectra of the coatings and the steel give us the opportunity to estimate the fraction of positrons implanted and transmitted through the coating, as well as the value of the effective mass absorption coefficients and implantation profiles of the positrons in the coatings [14,15]. Any linear annihilation parameter A (e.g. mean lifetime or intensity) is given as: $A = A_c f_c + A_m f_m$, where A_c and A_m are the characteristic values of A in the coating and in the metal, respectively. f_c and f_m are the fractions of positrons stopped in the coating and in the metal, respectively. Thus, measuring A as a function of the coating thickness x , the transmitted fraction, i.e., the relative number of positrons decaying in the steel, can be calculated as:

$$f_m(x) = \frac{A(x)-A_c}{A_m-A_c} \qquad (1)$$

while the implanted fraction in the coating is: $f_c = 1 - f_m$.

The transmitted fractions $f_m(x)$ have been determined by Eq. (1) using measured values of the mean lifetime and I_3 since these were the most reliable annihilation parameters. The results are plotted in Figure 4 for both coatings. Transmitted fractions $f_m(x)$ show nearly exponential behavior common to such experiments [14,15], characterized by an effective mass absorption coefficient (α). Then, to a good approximation:

$$\alpha = \frac{d \ln f_m(x)}{dx} \qquad (2)$$

Below a certain thickness value (x_0), the transmitted fraction differs significantly from pure exponential and Eq. (2) loses its validity. The value of x_0 for ^{22}Na positrons was found to be 5.7 mg/cm^2 [14] corresponding to coating thicknesses of approximately 30 μm and 60μm for the alkyd and epoxy coatings, respectively. The effective mass absorption coefficients estimated by Eq. (2) are listed in Table 2.

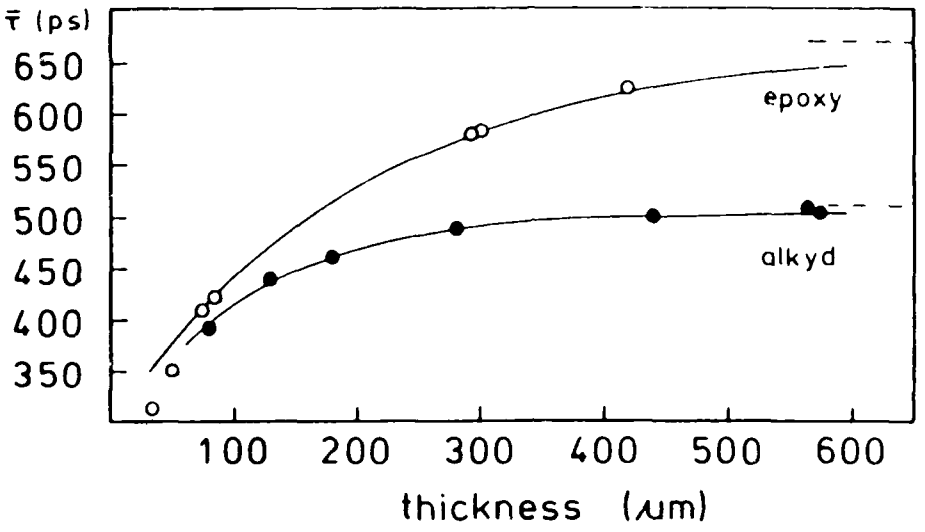

Figure 1. Positron mean lifetime as a function of coating thickness for the alkyd and epoxy coatings.

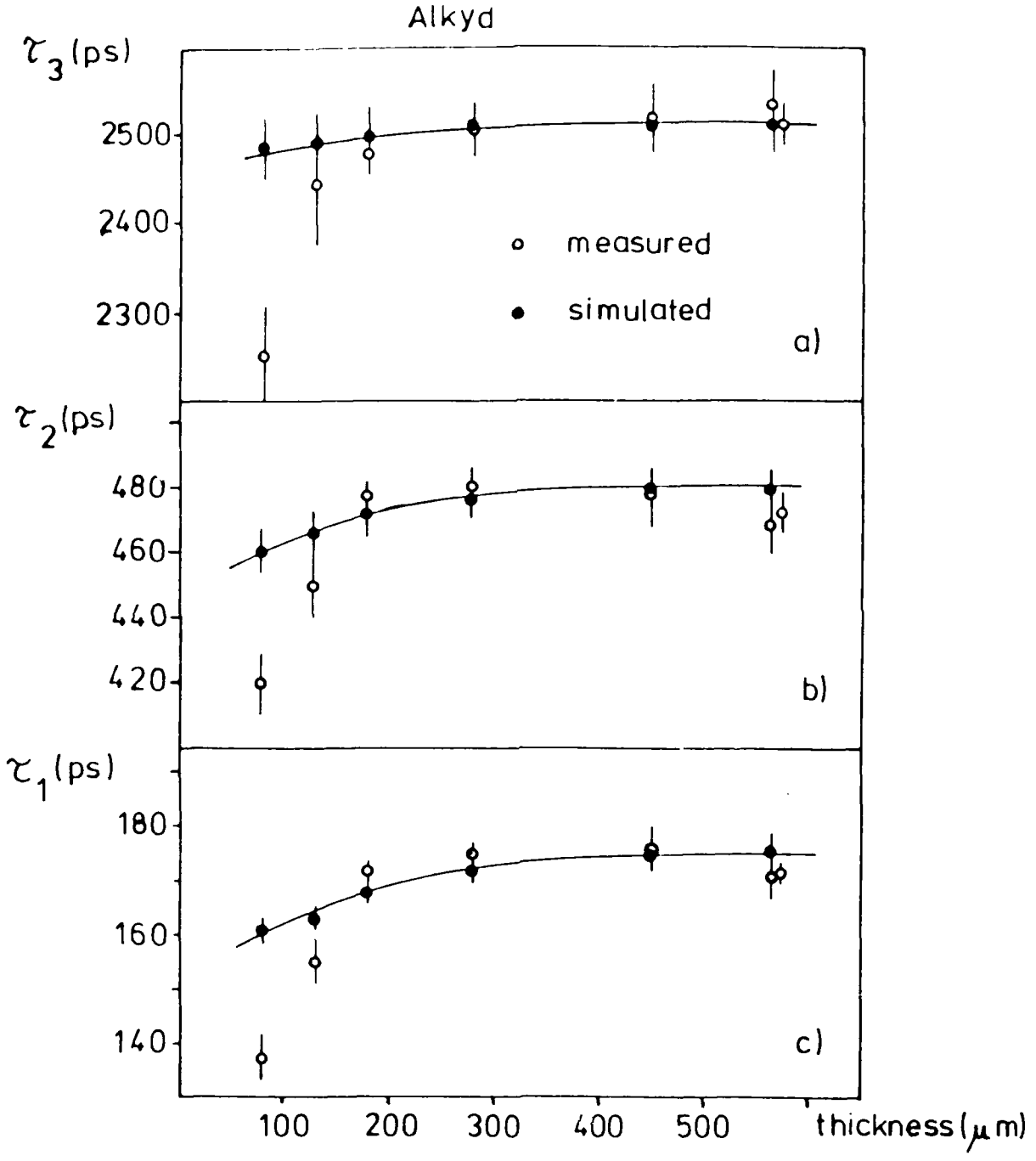

Figure 2A. Positron lifetimes of the three components as a function of thickness for the alkyd coatings. Full curves are the best exponential fits to the data points.

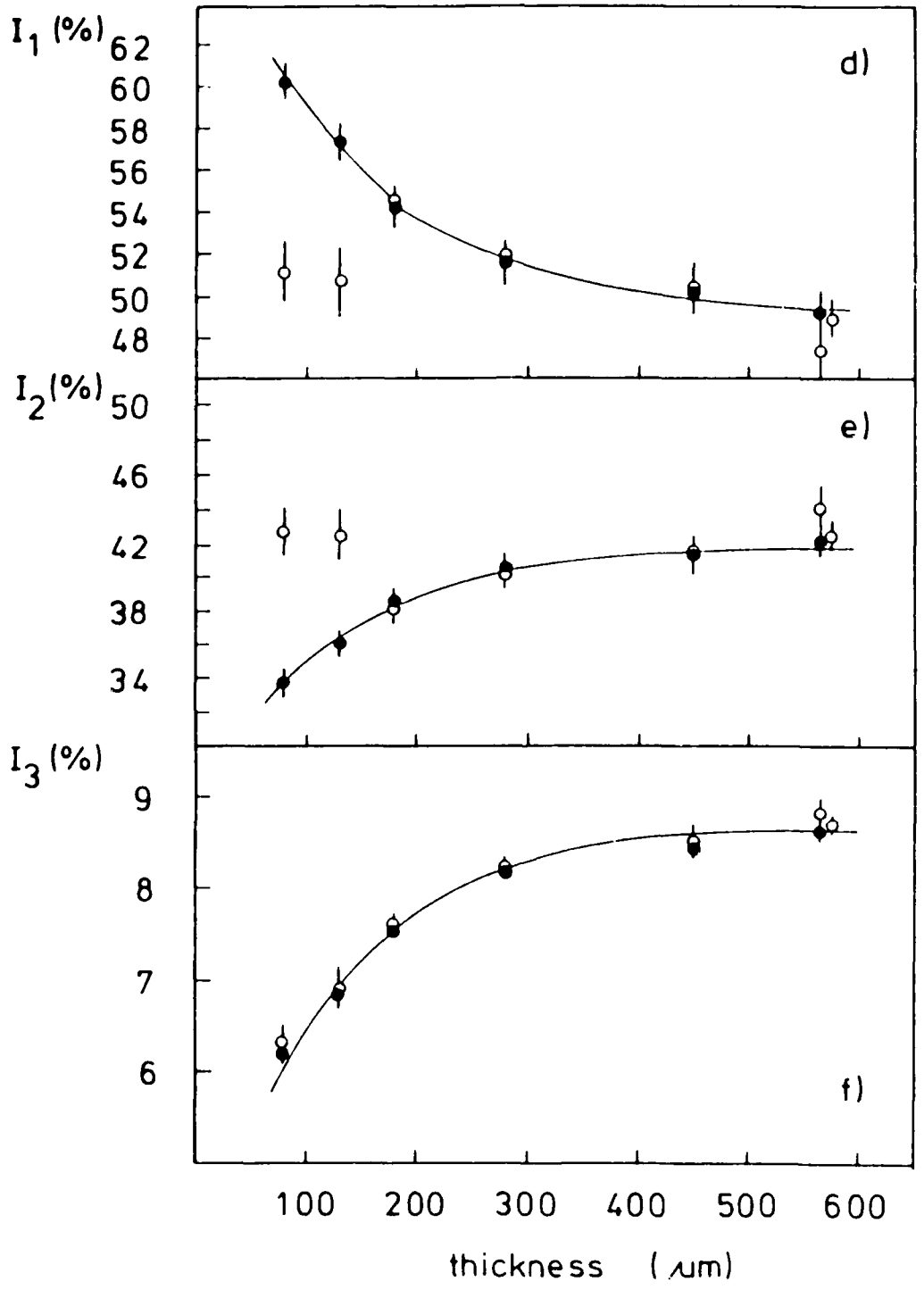

Figure 2B. Positron intensities for the three components as a function of thickness for the alkyd coating. Open circles are the measured values and the solid circles are the simulated values.

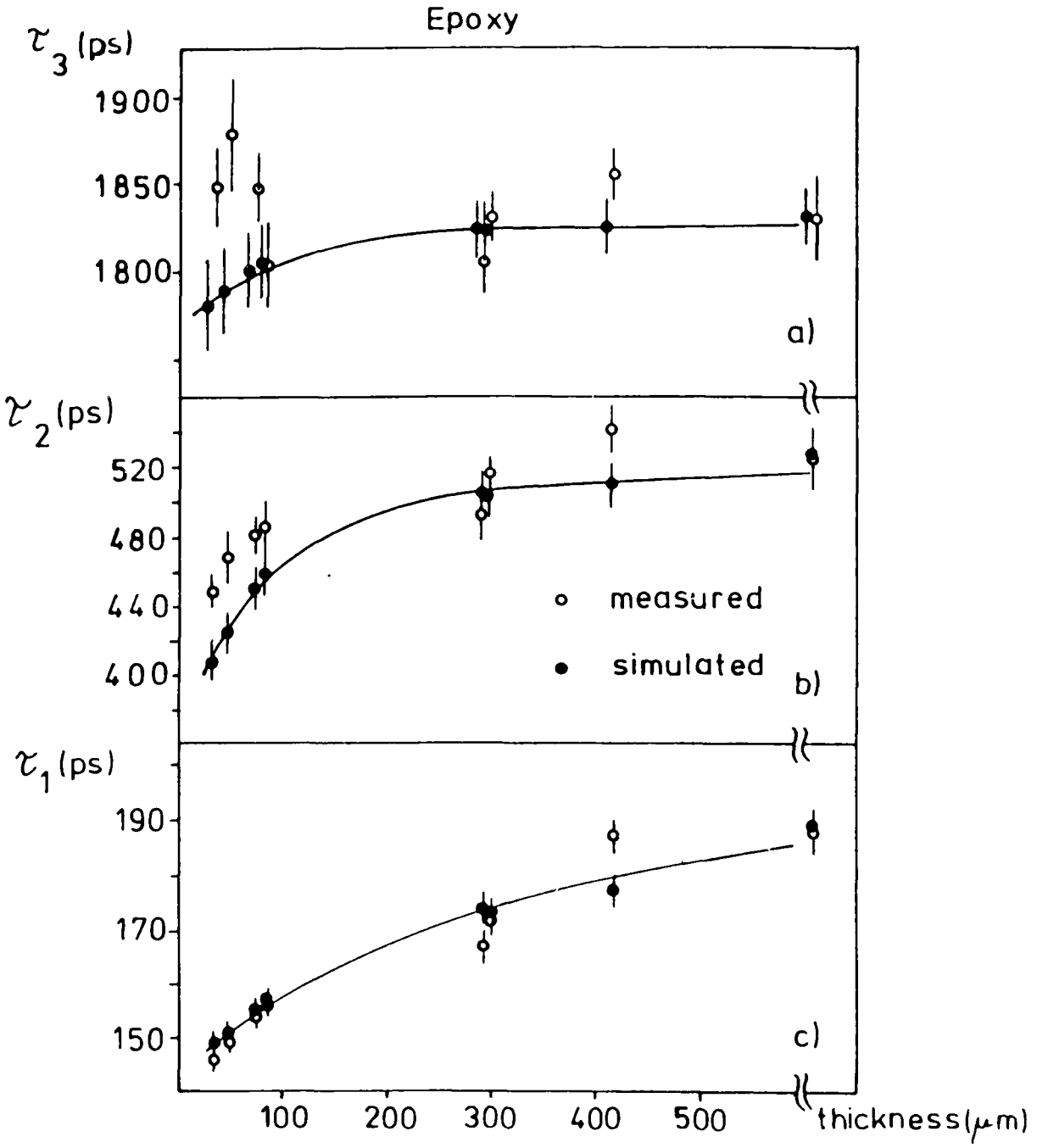

Figure 3A. Positron lifetimes of the three components as a function of thickness for the epoxy coating. Open circles are the measured values and the solid circles are the simulated values.

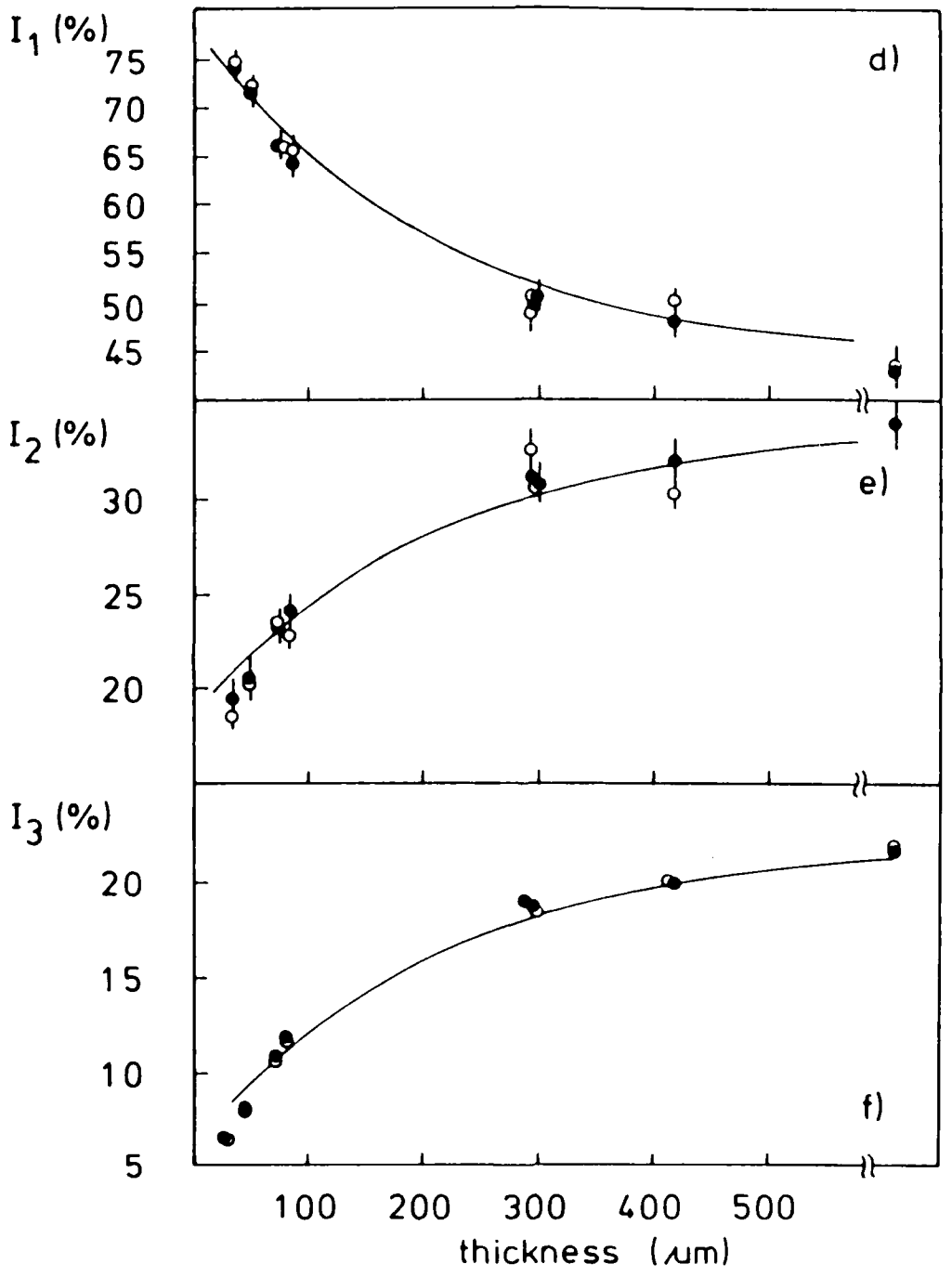

Figure 3B. Positron intensities for the three components as a function of thickness for the epoxy coating. Open circles are the measured values and the solid circles are the simulated values.

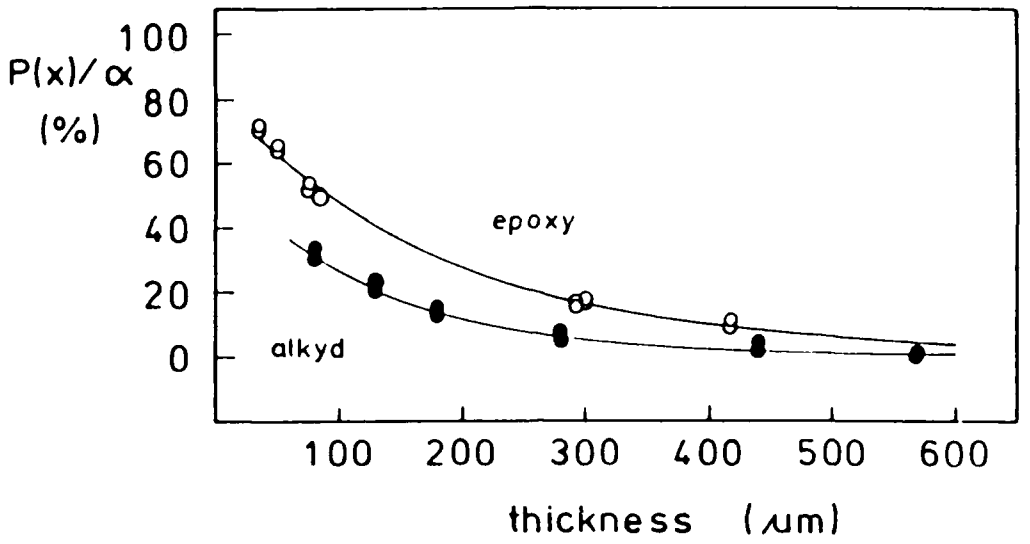

Figure 4. Transmitted intensities as a function of coating thickness for the alkyd and epoxy coatings.

Table 2. Effective mass absorption coefficients of positrons in the coatings

Material	α (cm^2/g)	$\delta\alpha$ (cm^{-1})
Alkyd	42.8 ± 2.8	86.9 ± 5.7
Epoxy	43.2 ± 1.8	48.8 ± 2.0

Equation (2) is useful if we want to determine the practical value of the effective mass absorption coefficient of positrons emerging from a ^{22}Na source for a given absorber (coating), reflector (steel) and geometry. The extracted value, however, may differ significantly from the intrinsic mass absorption coefficient of the absorber (coating) itself due to positron backscattering at the absorber-reflector interface which tends to increase the implanted and decrease the transmitted positron fractions [17]. Backscattering effects are also clearly manifested in our data. Neither mean lifetime nor I_3 converge towards the value of uncoated steel with decreasing thickness. The effect could be accounted for, in an approximate way, by introduction of an effective backscatter coefficient of positrons B at the coating/metal interface. B is that fraction of positrons reaching the metal surface which is reflected back into the polymer. The fraction of positrons stopping in the coating is then

$$f_c(x) = 1 - (1-B)\cdot\exp(-\alpha\cdot x) \quad , \tag{3}$$

if $x > x_0$. The mean lifetime and I_3 are then to a good approximation

$$\bar{\tau}(x) = \bar{\tau}_m + (\bar{\tau}_c - \bar{\tau}_m)\cdot f_c(x) \quad , \tag{4}$$

$$I_3(x) = I_3(\infty)\cdot f_c(x) \quad , \tag{5}$$

respectively, where $\bar{\tau}_m$ and $\bar{\tau}_c$ are the mean positron lifetimes for the metal and coating, while $I_3(\infty)$ is the asymptotic value of I_3 for high thickness values.

Curves in Figures 1, 2 and 3 of $\bar{\tau}$ and I_3 are the best fits to the data points with α and B as parameters. Extracted values of B (B = 0.41 and 0.26 for the alkyd and epoxy coatings, respectively) are in reasonable agreement with its value estimated according to Mackenzie et al. [13], B = 0.338 for steel. It should be pointed out that the above approximation strongly overestimates backscattering below x_0, which is clearly seen as a deviation of the

epoxy data from the fitted curve below 60 μm as shown in Figure 1. More detailed discussion of the backscattering effects was given elsewhere [4]. Transmitted fractions of positrons may be used to determine the positron implantation profile in the coatings:

$$P(x) = - \frac{1}{1-B} \cdot \frac{d\, f_m(x)}{d\, x} \quad . \qquad (6)$$

Figure 5 shows the derived implantation profiles.

Positron Annihilation

The positron lifetime spectra of the coating, as discussed previously, contains contributions both from the coating itself and from the metal substrate, unless the coating is thick enough to absorb all the injected positrons. Since the lifetime spectrum of the steel substrate can be described in terms of two lifetime components, the effect of the substrate shows up largely in the two shorter lifetime components of the coating. The contributions from the substrate diminish with increasing coating thickness and the spectrum converges towards that of the coating itself. The decreasing contribution from the steel is clearly shown by the decreasing intensity of the short-lived component and the concomitant increase of the intensities of the longer lifetime components. Since the shortest lifetime component is a sum of the contributions from the coating and the steel substrate, the measured lifetime value is sensitive to the coating thickness. Indeed it has been possible to model the thickness dependence of the short lifetime value, assuming it is a linear superposition of the short lifetime component of the coating and the mean lifetime characterizing the substrate [4].

An important question arising from these results is whether the variation in the lifetime of the longer lifetime components is a consequence of the simple superposition of the spectra of the coating and the substrate, or is due to a change in the nature of the coating with decreasing thickness. In order to address this question, computer-derived spectra have been compared with the measured spectra. The computer-derived spectra were generated using the experimental spectra of Table I and the experimental values of the implanted and transmitted positron fractions as determined from Eq. (1). The calculated five-component spectra were analyzed to three components characteristic of the coating, and the resulting lifetime and intensity values are shown as black dots in Figures 2 and 3. It is apparent from the simulated data that significant mixing of the steel lifetime components occurs in the case of τ_2 and even τ_3. This effect causes a systematic decrease of τ_2 and τ_3 from their values in the coating with decrease in coating thickness. These results show the importance of a knowledge of the positron depth distribution when studying coatings.

In the case of the epoxy coating, there was an excellent agreement between the measured and simulated values of the intensities and the short lifetime component over the entire thickness range as well as for τ_2 and τ_3 above 100 μm thickness. This result may be considered to support the concept that the measured spectra are simple linear superpositions of the coating and the metal spectra for coatings exceeding 100 μm in thickness.

Measured and simulated parameters, particularly τ_2 and τ_3 significantly deviate for thinner coatings. These observations cannot be ascribed to back-

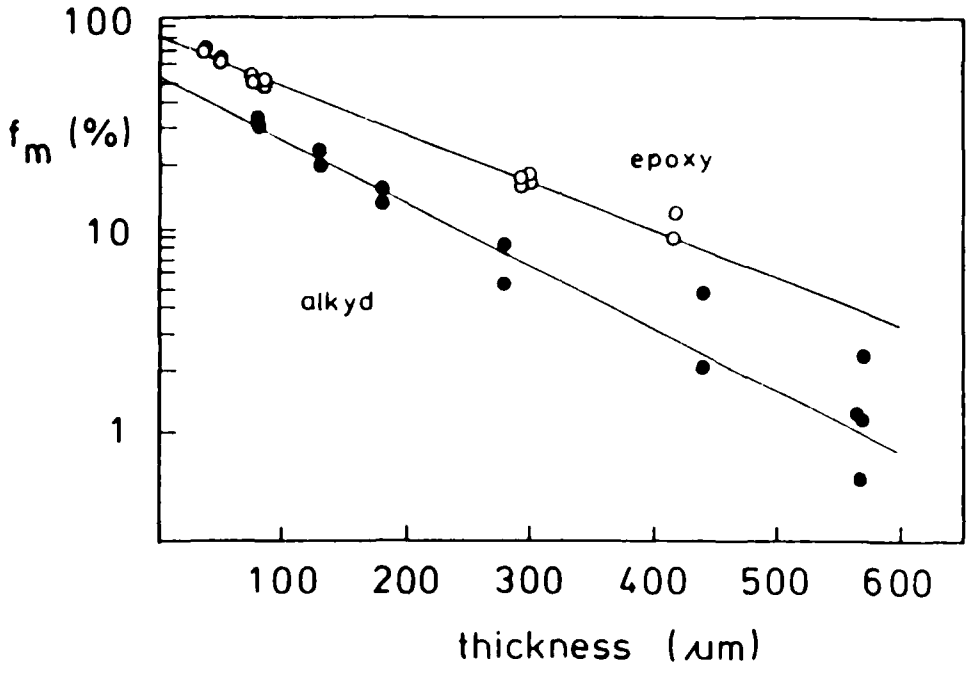

Figure 5. Positron implantation profiles in the alkyd and epoxy coatings.

scattering effects since the experimental implanted and transmitted fractions, which already contain the backscattered contributions, were used in calculating the simulated spectra. The disagreement between the measured and simulated spectra at low thicknesses are tentatively associated with changes in the coating morphology at thicknesses below 100 μm.

The lower calculated values of τ_2 and τ_3 for the thinner coatings in the case of the epoxy coating suggests an increase in the average size of both positron and positronium trapping sites with decreasing thickness. This effect is speculated to be caused by an inhomogeneous distribution of voids in the coating with a high concentration of voids existing in the vicinity of the metal/coating interface. Positrons sample this interfacial region, presumably containing the larger or more numerous voids, with higher probability as the coating is decreased in thickness.

The behavior of the lifetime parameters in the case of the alkyd coating is more complicated than in the case of the epoxy coating in that the values of τ_1, τ_2, τ_3, I_1 and I_2 deviate from the simulated values below 130 μm thickness. An increase in I_2 at the expense of I_1 for the thinner coatings suggests an increase of the free volume density at the metal/coating interface. The decrease in τ_1 is also in accord with this interpretation. The low values of τ_2 and τ_3 moreover suggest a decrease in the average size of free volumes near the interface with decrease in coating thickness.

The main difference between the annihilation properties of positrons in the alkyd and epoxy coatings arises in the long lifetime component. The value of this lifetime (τ_3 = 1800-2600 ps) shows that its origin is the formation of positronium in the coatings. The intensity values show that a much larger amount of positronium is formed in the epoxy coating than in the alkyd coating. Two interpretations are considered, either a more open structure (higher void content) in the epoxy coating or by a considerable inhibition of positronium formation in the alkyd coating.

ACKNOWLEDGMENT

Appreciation is expressed to the Office of Naval Research for partial support of the U.S.portion of the research.

REFERENCES

[1] H. Leidheiser, Jr., Proc. Intern. Conf. Localized Corrosion, Orlando, FL, June 1-5, 1987, H. Isaacs, Ed., Natl. Assoc. Corrosion Engrs., Houston, TX, in press.

[2] H. Leidheiser, Jr., Cs. Szeles, and A. Vértes, Nucl. Instr. Meth. Phys. Res. **A255**, 606 (1987).

[3] C. Szeles, A. Vértes, M. L. White, and H. Leidheiser, Jr., submitted to Nucl. Instr. Meth. Phys. Res.

[4] K. Suvegh, C. Szeles, A. Vértes, M. L. White, and H. Leidheiser, Jr., J. Radioanal. Nucl. Lett. **117**, 183 (1987).

[5] Positron Solid State Physics, Eds. W. Brandt and A. Dupasquier, North-Holland: Amsterdam, 1983.

[6] Positron Annihilation, Eds. P. C. Jain, R. M. Singru and K. P. Gopinathan, World Scientific: Singapore, 1985.

[7] M. Eldrup in: Ref. 6, p. 644.

[8] A. P. Mills, Jr., in: Ref 6, p. 432.

[9] A. Dupasquier and A. Zecca, Riv. Nuovo Cimento **8**, 1 (1985).

[10] J. H. Jilek, Prog. Org. Coat. **5**, 97 (1977).

[11] J. J. Singh, W. H. Holt, and W. Mock, Jr., Nucl. Instr. Meth. Phys. Res. **201**, 485 (1982).

[12] P. Kirkegaard, M. Eldrup, O. E. Mogensen, N. J. Pedersen, Comp. Phys. Commun. **23**, 307 (1981).

[13] I. K. Mackenzie, C. W. Schulte, T. Jackman, J. L. Campbell, Phys. Rev. **A7**, 135 (1973).

[14] H. E. Hansen, S. Linderoth, and K. Petersen, Appl. Phys. A **29**, 99, (1982).

[15] A. Bisi, L. Braicovich, Nucl. Phys. **58**, 171 (1964).

[16] M. Bertolaccini, L. Zappa, Nuovo Cimento **52B**, 487 (1967).

[17] S. Linderoth, H. E. Hansen, B. Nielsen, and K. Petersen, Appl. Phys. A **33**, 25 (1984).

Effect of Alkali Metal Hydroxides on the Dissolution Behavior of a Zinc Phosphate Conversion Coating on Steel and Pertinence to Cathodic Delamination

André J. Sommer and Henry Leidheiser, Jr.

Published in CORROSION 43(11), 1987, pp.661-65.

Effect of Alkali Metal Hydroxides on the Dissolution Behavior of a Zinc Phosphate Conversion Coating on Steel and Pertinence to Cathodic Delamination

ABSTRACT

Raman microprobe spectroscopy, scanning electron microscopy (SEM), energy dispersive spectroscopy (EDS) and wet chemical methods of analysis were successfully used to determine the effects of high pH environments on zinc phosphate conversion coatings. The more rapid dissolution of phosphate ions from the phosphate coating was pH dependent. At a pH of 12.5, phosphate ions were more rapidly dissolved from the phosphate coating while at 11.5 and 13.5 pH, zinc ions were more rapidly dissolved from the coating. Raman spectra confirmed the more rapid dissolution of the phosphate ions was a result of zinc oxide formation on the surface of the original phosphate conversion coating. The cation of the alkaline environment also proved to be an important factor in the dissolution of the phosphate conversion coating. Sodium hydroxide dissolved the phosphate coating at the greatest rate followed by hydroxides of potassium, cesium and lithium. This cation dependence was related to the number of precipitation products formed in the different alkaline solutions.

INTRODUCTION

Cathodic delamination is a term used to describe the adhesion loss of an organic coating from a cathodically protected metal. The origin of the failure can be traced to defects or voids in the organic coating, which allows oxygen and water to come in contact with the metal. Cathodic reduction of oxygen to produce hydroxyl ions increases the pH in the electrolyte adjoining the defect and disrupts bonding between the organic coating and the metal substrate. Bond failure may occur via alkali reaction with the organic coating or by dissolution of the inorganic species present at the organic coating/metal substrate interface.

Before being coated with an organic coating, the metal substrate is often phosphate conversion coated with iron and/or zinc phosphates. Wiggle, Smith and Petrocelli [1] first noted that zinc phosphate conversion coatings dissolve in the high-pH environments formed under a coating when the metal surface serves as the cathode. Later studies by Roberts et al. [2] demonstrated that phosphorus was selectively removed from the phosphate coating when exposed to sodium hydroxide solutions. Recently, Uchida and Deguchi [3] and Van Ooij and De Vries [4] reported similar findings in commercial paint systems. Van Ooij and De Vries interpreted XPS studies to show that hydroxide ions exchange with phosphate ions in the first few layers of the phosphate coating. A number of questions still needing answer are [3]: (1) Is the selective dissolution of phosphorus pH dependent? (2) Why is the phosphate ion more rapidly dissolved from the phosphate coating? (3) What effect do cations have on the dissolution of the phosphate coating? and (4) What corrosion products or dissolution products are formed?

The purpose of this investigation is to answer these questions and seek a better understanding of high-pH effects on phosphate conversion coatings. This investigation is not at all comprehensive but is offered to complement the work of authors previously cited and to confirm some of the interpretations they have made.

The primary investigative technique used in this study was Laser Raman Microprobe Spectroscopy (LRMS). The instrument and the concomitant strengths and inadequacies of the technique have been discussed elsewhere [5,6]. A strength of LRMS pertinent to this investigation is that the technique provides molecular characterization on a microscopic scale at ambient conditions. The inadequacies of LRMS have been counteracted by measurements using energy dispersive spectroscopy (EDS), scanning electron microscopy (SEM), and wet chemical methods of analysis.

EXPERIMENTAL

Influences of the following two variables on the dissolution of zinc phosphate conversion coatings were investigated: (1) the pH of the aqueous environment and (2) the cation present in that environment. The influence of pH was determined by exposing zinc phosphated steel samples to 0.01M, 0.1M, and 1.0M sodium hydroxide solutions. Hydroxide solutions (0.1M) of lithium, sodium, potassium, and cesium were used to determine the effect of cations on phosphate dissolution.

Zinc-phosphated steel samples (Parker 210) obtained from Parker Surface Treatment Products were cut into 2.5-cm squares. Back sides of the phosphated steel panels were marked before cutting so that the cut samples had the same sides exposed to the test solutions. Only those samples cut from the center of the panel were used.

Three sets of six samples each were exposed to the various hydroxide solutions by clamping the panel to the base of an O-ring ball joint cell. At intervals of 10, 20, 30, 40, 50 and 60 min, the samples were removed, rinsed lightly with distilled water and allowed to dry. A small portion of the solution volume was then analyzed for orthophosphate and divalent zinc by a colorimetric method and atomic absorption spectroscopy, respectively. Samples exposed to the hydroxide solutions for a total of 1 h were analyzed by LRMS, SEM, and EDS.

A model experiment was conducted to determine the corrosion products generated by exposing the phosphated steel to high-pH environments. Zinc phosphate tetrahydrate was pressed into a pellet and exposed to 1.0M NaOH for 1 h. Corrosion products generated in this manner were identified by comparing Raman spectra of known materials to those spectra recorded for the corrosion products.

RESULTS

Model Experiment

Results of the model experiment and Raman analysis of the subsequent reaction products formed are shown in Figure 1. The Raman spectrum of the zinc phosphate tetrahydrate pellet exposed to 1.0M NaOH exhibited three bands located at 435, 980 and 1083 cm^{-1}. Reference Raman spectra of zinc oxide, hydrozincite, hydroxyapatite, and hopeite are also presented for comparison.

Wet Chemical Analysis

Table 1 lists the measured phosphate ion dissolution rate in μmol/l min for samples exposed to 0.01M, 0.1M and 1.0M NaOH and 0.1M hydroxide solutions of lithium, potassium, and cesium. Rates were obtained from the slope of the least squares fit of the data and confidence limits were calculated at the 95% level. The table also lists these dissolution rates normalized to that measured for 0.01M NaOH and 0.1M LiOH. The data presented show that the phosphate dissolution rate increased upon increasing the pH. Changing the cation of the hydroxide solution also had a significant effect on phosphate dissolution. Sodium hydroxide was 4.1 times more effective in dissolving phosphate ions from the phosphate coating than LiOH and ~1.6 and 2.6 times more effective than KOH and CsOH, respectively.

Table 1 - Phosphate Ion Dissolution Rate (μmols/l min)

	NaOH		
Rate	0.01M	0.1M	1.0M
Measured	0.04 ± 0.02	5.8 ± 0.4	72.0 ± 0.5
Normalized to 0.01M NaOH	1.0	72	900

Rate	LiOH 0.1M	NaOH 0.1M	KOH 0.1M	CsOH 0.1M
Measured	1.4 ± 0.2	5.8 ± 0.4	3.7 ± 0.5	2.2 ± 0.3
Normalized to 0.1M LiOH	1.0	4.1	2.6	1.6

Figures 2 and 3 are plots of the mol ratio of zinc ions to phosphate ions in solution as a function of exposure time for the various hydroxide solutions. Confidence limits for the ratios were on average ± 0.2 and were calculated at the 80% confidence level.

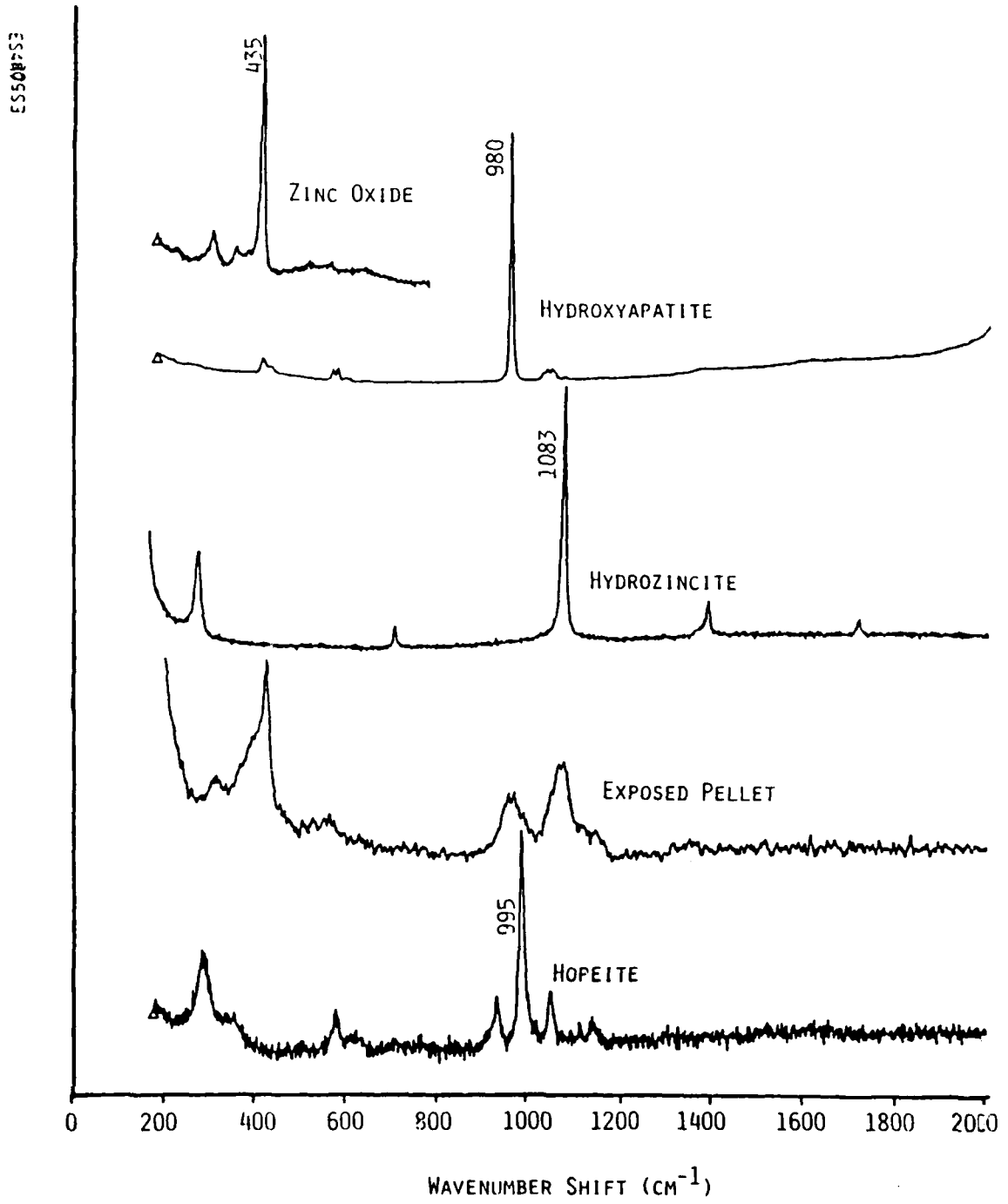

Figure 1. The Raman spectra of zinc oxide, hydroxyapatite, hydrozincite, hopeite and the exposed pellet after exposure to 1M NaOH for 1 h at room temperature.

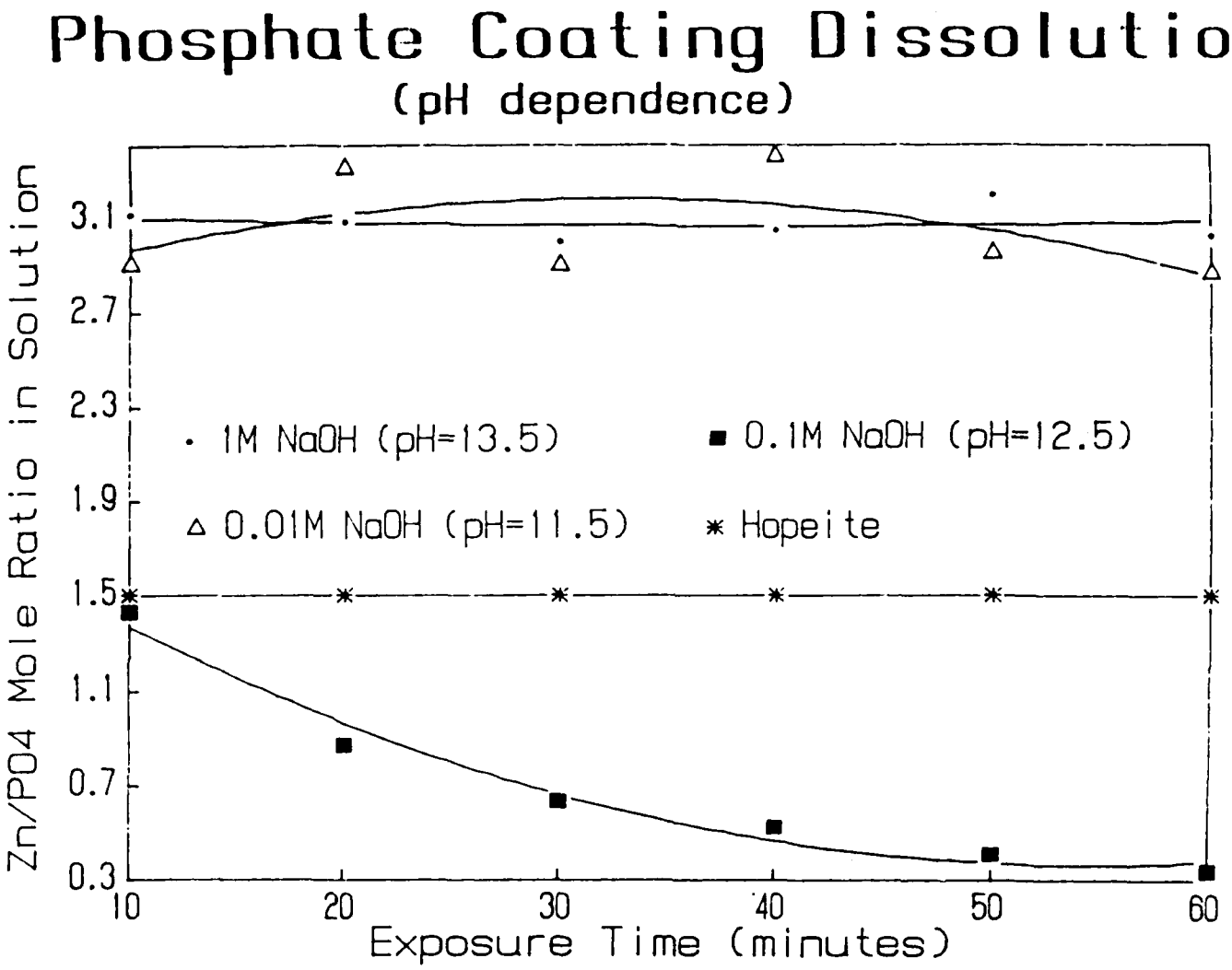

Figure 2. The mole ratios of zinc ion/phospate ion in solution after exposure of the phosphate to 0.01, 0.1 and 1M NaOH.

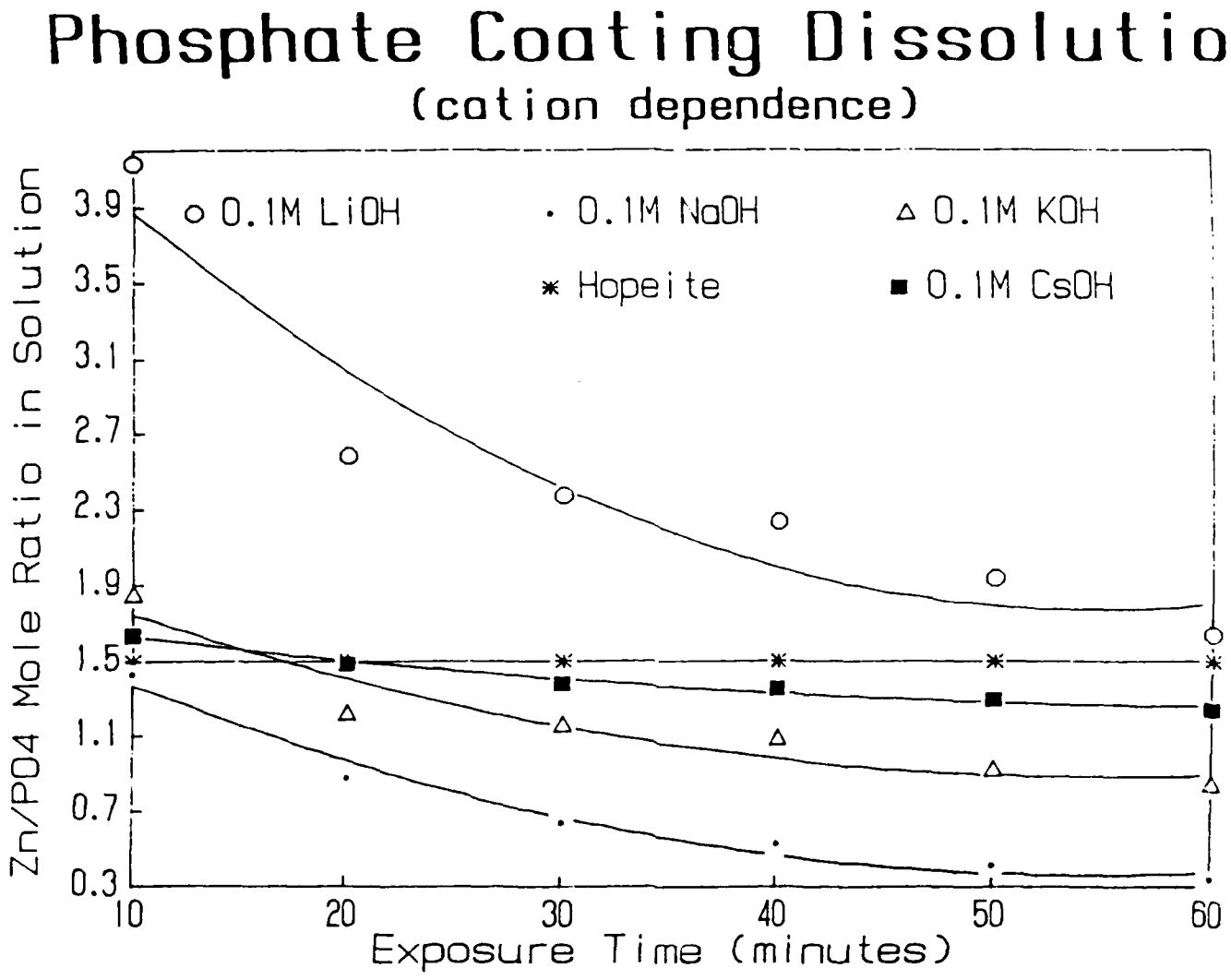

Figure 3. The mole ratios of zinc ion/phosphate ion in solution after exposure to 0.1M solutions of LiOH, NaOH, KOH and CsOH.

One-Hour Exposure

Results of SEM, EDS and LRMS analyses on those samples exposed for 1 h are summarized in Table 2. SEM analysis showed the formation of a precipitate on the surface of samples exposed to 0.1M NaOH and 0.1M KOH. Those samples exposed to 0.01M NaOH, 0.1M LiOH and 0.1M CsOH showed surface morphology characteristic of a normal zinc phosphate coating. The sample exposed to 1.0M NaOH showed that all of the phosphate crystals had been dissolved from the steel surface.

Table 2 - SEM, EDS, and Raman Analysis of Samples Exposed for 1 h

	NaOH			LiOH	KOH	CsOH
Analysis	0.01M	0.1M	1.0M	0.1M	0.1M	0.1M
SEM	NP[a]	ppt	--	NP	ppt	NP
EDS	NP	-P	-P,-Zn +Fe	NP	-P	-P
Raman	NP	NP[b]	--	NP	NP[b]	NP

[a]NP = normal zinc phosphate.
[b]The loss of signal/noise ratio in spectra.

EDS spectra of samples exposed to 0.1M solutions of NaOH, KOH, and CsOH showed that phosphorus was removed from the coating while the amount of zinc in the coating remained unchanged. Samples exposed to 0.01M NaOH and 0.1M LiOH yielded EDS spectra with phosphorus and zinc peak intensities characteristic of a normal zinc phosphate coating. EDS spectra of samples exposed to 1.0M NaOH showed that most of the phosphorus and zinc had been removed from the coating. This sample also exhibited a large signal for iron.

Raman spectra yielded bands characteristic of hopeite for all the samples except those exposed to 0.1M NaOH, 0.1M KOH and 1.0M NaOH. Raman spectra could not be recorded for the latter sample. The spectra recorded for samples exposed to 0.1M solutions of NaOH and KOH exhibited a decrease in the signal to noise ratio of all peaks associated with hopeite.

Four-Day Exposure

Results of SEM, EDS, optical microscopy and LRMS are summarized in Table 3. SEM and EDS analyses showed the formation of a precipitate on the original phosphate coating and a loss of phosphorus from that coating for each of the samples exposed to the various hydroxide solutions. When viewed under an optical microscope, one, two, three and four distinct phases were detected in the coatings of samples exposed to 0.1M solutions of NaOH, KOH, LiOH and CsOH, respectively. Raman analysis of these phases detected zinc

oxide (samples exposed to NaOH), zinc oxide, and an orthophosphate of potassium, iron and zinc (samples exposed to KOH), zinc oxide, vivianite, hydrozincite and Fe_3O_4 (samples exposed to LiOH) and vivianite, hydrozincite, ferric phosphate and an orthophosphate of cesium, iron and zinc (samples exposed to CsOH).

DISCUSSION

Zinc Phosphate - Alkali Reaction Products

Results of an earlier investigation in which the zinc-phosphated steel samples were characterized by LRMS showed that the phosphate coating was predominantly hopeite [7]. Hopeite, $Zn_3(PO_4)_2{:}4H_2O$, is a zinc phosphate tetrahydrate for which the Raman spectrum is shown in Figure 1. Figure 1 also shows the Raman spectrum of a zinc phosphate tetrahydrate pellet exposed to 1.0M NaOH for 1 h and the Raman spectra of zinc oxide, hydrozincite, and hydroxyapatite. Raman bands in the spectrum of the exposed pellet can be assigned to zinc oxide (435 cm^{-1} shift), hydroxyapatite (980 cm^{-1} shift), and hydrozincite (1083 cm^{-1} shift).

The Raman band for zinc oxide is characteristic of lattice vibrations within the zinc oxide crystal and/or zinc-oxygen bonding modes. Hydroxyapatite [$Zn_{10}(OH)_2(PO_4)_6{:}nH_2O$] is a basic phosphate of zinc, whose characteristic Raman band is assigned to the symmetric stretch of the phosphate tetrahedra. Symmetric stretching of carbonate ions give rise to the major Raman band in hydrozincite [$2ZnCO_3{:}3Zn(OH)_2$], a basic carbonate of zinc. Band broadening in the spectrum of the exposed pellet results from the polycrystalline nature of the reaction products. Polarization contributions from different crystal orientations tend to broaden the Raman line shapes.

Effects of pH

Data presented in Table 1 demonstrate that the rate of phosphate ion removal from the phosphate coating is increased by increasing the pH, a fact noted in a previous study by Roberts et al. [2]. Based on the chemical formula for hopeite [$Zn_3(PO_4)_2{:}4H_2O$], uniform dissolution of the phosphate coating dictates that the zinc ion to phosphate ion mol ratio in solution be ~1.5. Ratios smaller than 1.5 indicate that phosphate ions are being more rapidly dissolved from the coating, while ratios greater than 1.5 indicate more rapid dissolution of zinc ions from the coating. The mol ratios of zinc ion to phosphate ion in solution plotted as a function of exposure time and pH in Figure 2 clearly demonstrate that zinc ions are more rapidly dissolved from the coating in 0.01M and 1.0M NaOH solutions while phosphate ions are more rapidly dissolved in 0.1M NaOH solutions. Phosphate conversion coatings used in this study were primarily comprised of hopeite. However, the possibility does exist that small amounts of phosphophyllite, $Zn_2Fe(PO_4)_2{:}2H_2O$, may also be present. Uniform dissolution of this phosphate yields zinc ion to phosphate ion ratios in solution of ~1.0. In all cases, the ratios are either well below or above this value; thus, zinc or phosphate ions are dissolved at a greater rate from the phosphate coating, depending upon the pH of the solution. To determine why these have different rates of dissolution in solutions of differing pH, SEM, EDS, and LRMS analyses were conducted on those samples exposed for 1 h.

Results of these analyses provided little information except for the fact that a precipitate had formed on the sample exposed to 0.1M NaOH and that the EDS results confirmed or paralleled the wet chemical results. Lower signal to noise ratios in Raman spectra of samples exposed to 0.1M NaOH can be attributed to the increased Rayleigh scattering by the precipitate on the

phosphate coating surface. The amount of precipitate was insufficient to permit a clear identification, therefore samples were exposed to 0.1M NaOH for four days so more precipitate would form. SEM photomicrographs of these latter samples confirmed that a greater amount of precipitate had been deposited and subsequent Raman analysis identified the precipitate as zinc oxide. Results presented earlier and in the foregoing discussion show that phosphate conversion coating dissolution is very dependent upon the pH of the solution. Low P to Zn ratios in the surface of zinc phosphate exposed to 0.1M NaOH observed in previous studies were confirmed by Raman analysis performed in this study to be a consequence of zinc oxide formation on the coating surface [2,4]. Differing rates of dissolution for phosphate and zinc were also found to be pH dependent and can be explained as follows. In solutions with a pH close to that of 0.01M NaOH (11.5) the zinc phosphate conversion coating is very slowly dissolved. Zinc ions are preferentially removed from the coating by the formation of soluble zincate complexes of the form $[(Zn(H_2O)_m(OH)_n)]^{2-n}$ [8]. As the pH increases towards 0.1M NaOH (12.5), the solubility product constant of zinc oxide is exceeded and zinc oxide is precipitated onto the surface. Since phosphate ions continue to be solvated, the precipitation of zinc oxide leads to a lower P to Zn ratio on the surface and to a lower Zn^{2+} to PO_4^{-3} ratio in solution. Increasing the pH further to that of 1.0M NaOH (13.5) solubilizes the zinc oxide precipitate and zincate complexes of higher order are formed in solution.

Effects of Cations

Leidheiser and Wang [9] have shown that cations play an important role in cathodic delamination. The cations act as charge carriers and provide charge balance for the OH^- ions formed by cathodic delamination. The combined effect of hydroxide anions and cations on phosphate coating dissolution had to be determined since companion studies of cathodic delamination were conducted with zinc phosphated steel substrates [10].

Data presented in Table 1 demonstrate that cations also affect phosphate coating dissolution. The most surprising result is that sodium ions are approximately 1.6, 2.6 and 4.1 times more effective in phosphate coating dissolution than potassium, cesium, and lithium, respectively. The data plotted in Figure 3 show that phosphate ions are more rapidly dissolved from the phosphate coating for sodium, potassium, and cesium (i.e., ratios below 1.5), whereas zinc ions are more rapidly dissolved when the ion of the alkali solution is lithium (i.e., ratios above 1.5).

Results of SEM, EDS, and LRMS analysis of the samples exposed for 1 h, listed in Table 2, provided little information as to why the phosphate coating dissolved differently in the different alkaline media. EDS analysis confirmed results obtained via wet chemical analysis, except for those samples exposed to LiOH. In this case small changes in the phosphate coating detected by wet chemical methods would not be detected by EDS analysis, which is at best a semiquantitative technique. The only significant difference between the samples was that a precipitate formed on samples exposed to 0.1M solutions of NaOH and KOH. Details of this precipitate formation were discussed previously for sodium and it is expected that similar mechanisms are occurring in samples exposed to KOH. Close examination of the SEM photomicrographs of samples exposed to KOH showed that the edges of the phosphate crystals were more rounded when compared to those phosphate crystals exposed

to NaOH. This observation suggests that KOH attacks the phosphate crystals more vigorously than NaOH. However, this suggestion conflicts with wet chemical results. A possible explanation for these observations is that the phosphate, once dissolved from the coating, may precipitate in another form. Again samples were exposed to the various hydroxide solutions for four days so that more information could be gained.

Results of SEM and EDS analyses summarized in Table 3 for those samples exposed for four days indicate that a precipitate formed on the surface of each of the samples and that in each case the surface lost phosphorus. Observation of these surfaces under an optical microscope at 100X revealed differences consistent with the dissolution rate order seen on changing the cation of the alkaline exposure solution. Samples exposed to NaOH exhibited one phase which was later identified as zinc oxide by LRMS. Exposure of the phosphated steel to KOH produced two phases identified by LRMS as zinc oxide and an orthophosphate of potassium, iron and zinc. Samples exposed to LiOH and CsOH exhibited three and four phases as concluded from optical microscopy. Subsequent Raman microanalysis of these phases confirmed the formation of vivianite (a ferric phosphate), Fe_3O_4, zinc oxide and hydrozincite for samples exposed to LiOH; ferrous phosphate, vivianite, hydrozincite and an orthophosphate of cesium, iron, and zinc for those samples exposed to CsOH.

Table 3 - SEM, EDS, and Raman Analysis of Samples Exposed for 4 Days

Analysis	LiOH 0.1M	NaOH 0.1M	KOH 0.1M	CsOH 0.1M
SEM	ppt	ppt	ppt	ppt
EDS	-P	-P	-P	-P
Optical Microscopy	3 phases	1 phase	2 phases	4 phases
LRMS (Raman)	vivianite, Fe_3O_4, ZnO, hydrozincite	ZnO	ZnO ortho-phosphate	vivianite, hydrozincite, orthophosphate, $FePO_4:2H_2O$

Based on the foregoing results, the effect of cations on phosphate dissolution appears to be related to the solubility of precipitates formed after dissolution of the original zinc phosphate coating. Generally, the larger the cation, the more numerous are its insoluble salts; a fact that would account for the order of the dissolution rates on changing the cation from sodium to cesium but would not explain the dissolution rate observed in LiOH [8]. The reason for this disparity may reside in the fact that the chemistry involved in the model system investigated is very complex. Determining the effects of hydroxide anions and cations on phosphate coating dissolution was

essential because this particular phosphate coating system was to be used in future studies of cathodic delamination. A phosphate coating system which would be more suitable for determining the effects of cations on phosphate coating dissolution would be an iron phosphate coating in a controlled atmosphere. In the latter system, the number of ions in solution would be decreased, thereby making the dissolution chemistry a littler easier to deal with. The controlled atmosphere (argon or nitrogen purge) would eliminate the carbonate anion along with its insoluble dissolution products.

CONCLUSIONS

The data and observations clearly show that dissolution and selective solvation of ions from the phosphate conversion coating are pH dependent. Furthermore, the dissolution rate of the phosphate coating is strongly dependent on the cation present in the aqueous environment. Future interests are to determine whether any of the effects or mechanisms observed in this investigation play an important role in cathodic delamination phenomena and in real life systems. Finally, the focus of this paper has limited the presentation of all the Raman results. These results have been substantiated and reported elsewhere [10].

Acknowledgments

The authors are grateful to the Office of Naval Research for providing support for this investigation. The authors are also grateful to K. Korinek of Parker Surface Treatment Products for supplying the phosphated-steel samples. F. Adar of Instrtuments SA is also to be thanked for her assistance in interpreting the Raman spectroscopic results.

REFERENCES

[1] R.R. Wiggle, A.G. Smith, J.V. Petrocelli, J. Paint Tech., Vol. 40, p.174, 1968.

[2] T.R. Roberts, J. Kolts, J.H. Steele, Jr., SAE Trans. 89, p.1749, 1980.

[3] K. Uchida, T. Deguchi, Nisshin Steel Co. Report #667.613, Nisshin Steel Co., Chiba, Japan, p.32, 1983.

[4] W.J. Van Ooij, O.T. De Vries, 10th Inter. Conf. on Organic Coatings Science and Technology, A.G. Patsis, State University of New York, New Paltz, NY, 1984.

[5] P. Dhamelincourt, F. Wallart, M. Leclerq, A.T. N'Guyen, D.O. Landon, Anal. Chem., Vol. 51, p.414, 1979.

[6] M. Delhaye, P. Dhamelincourt, J. Raman Spectroscopy, Vol. 3, p.33, 1975.

[7] A.J. Sommer, H. Leidheiser, Jr., Microbeam Analysis, A.D. Romig, J.I. Goldstein, Eds., San Francisco Press, Inc., San Francisco, CA, pp.111-14, 1984.

[8] F.A. Cotton, G. Wilkinson, Advanced Inorganic Chemistry, 4th ed., John Wiley and Sons, Inc., New York, NY, p.752, 1980.

[9] H. Leidheiser, Jr., W. Wang, Corrosion Control by Organic Coatings, H. Leidheiser, Jr., Ed., National Association of Corrosion Engineers, Houston, TX, p.70, 1981.

[10] A. Sommer, Ph.D. Thesis, Lehigh University, University Microfilms, Bethlehem, PA, 1985.

END

DATE

FILMED

8-88

DTIC